

A model for NL and SL decays by $\bar{B}^0 \rightarrow D^{**}$ transitions with $BR(j = 1/2) \ll BR(j = 3/2)$ using the *LLSW* scheme

Alain Le Yaouanc, Jean-Pierre Leroy, and Patrick Roudeau
Université Paris-Saclay, CNRS/IN2P3, IJCLab, 91405 Orsay, France
(Dated: 12 mai 2021)

We present a model for the vector and axial form factors of the transitions $\bar{B}^0 \rightarrow D^{**}$ in good agreement with the presently available data and based on the present theoretical knowledge, combining a) the safe lattice QCD predictions at $m_Q = \infty$ and $w = 1$; b) the predictions at general w of a relativistic, covariant quark model at $m_Q = \infty$, including the well tested Godfrey and Isgur spectroscopic model and which agrees with lattice QCD at $w = 1$; c) the constraint of Bjorken and Neubert relating Semi-leptonic (SL) and Class I Non-leptonic (NL) decays, which shows that $\bar{B}^0 \rightarrow D_0(2300)^+ \pi^-$ strongly constrains $\tau_{1/2}(w)$ to be much smaller than $\tau_{3/2}(w)$, in agreement with the theoretical expectation; d) the general HQET expansion which constrains the $1/m_Q$ corrections (cf [1], denoted hereafter as *LLSW*).

An important element in the understanding of data is the large contribution of virtual $D_V^{(*)}$ to the broad structures seen in SL decays at low $D^{(*)}\pi$ masses - which makes it difficult to isolate the broad resonances denoted as $D_{1/2}$ in the following.

I. INTRODUCTION

There is insufficient knowledge of both non-leptonic (NL) and semi-leptonic (SL) transitions to charmed orbital excitations, generically termed as D^{**} . The latter (SL) are especially interesting

1) in themselves,

for a) striking theoretically expected features which contradict the naive idea of strong similarity between SL transitions to $j = 1/2$ and $j = 3/2$ D^{**} ,

and b) for the apparent contradiction between this expectation and the presently widespread interpretation of experimental data on broad states, a contradiction which we claim to have resolved by the interplay of the possibly large D_V^* background [2].

2) for some applications, like the background to $\bar{B} \rightarrow D^{(*)} \ell^- (\tau^-) \bar{\nu}_{\ell(\tau)}$. Ultimately, one would like to have a description of the full system of semi-leptonic $\bar{B} \rightarrow D^{**}$ form factors, but this appears a hard task.

Indeed, there are no full calculations of the latter from first principles, as are provided in simpler cases by lattice QCD. Presently, the latter gives results only at $m_Q = \infty$ and $w = 1$. The reasons are given below, Section II.

On the other hand, the experimental data are scarce : total branching ratios, some points in the $d\Gamma/dw$ of certain transitions... Then, as explained in more details below, Sections II and VIII, a more complicated path is to be followed, combining theoretical inputs and experience, the former being used in addition in several different ways.

We want indeed to use the very useful general ideas of the extensive analyses of [3–5] [?] relying on their HQET analysis, but to take into account

1) **quantitative dynamical results at $m_Q = \infty$** of lat-

tice QCD (completed by quark models in the Bakamjian-Thomas (BT) approach) as well as

2) the **very important experimental measurements of $\bar{B}^0 \rightarrow D_0(2300)^+ \pi^-$** which constrain strongly the transition to $j = 1/2$ to be small, both of them having been disregarded in the *LLSWB* analyses.

Finally we underline the very important role of the D_V^* background in the SL decays, which we have already emphasized in [2], and which, we think, has not been fully taken into account up to now.

All these elements, taken together, change drastically the conclusions with respect to the ones of the above mentioned analyses, especially the claim that the Isgur-Wise (IW) functions are roughly equal at $w = 1$, as we explain now.

The *LLSW* approach [3], provides a framework to parameterize $1/m_Q$ corrections in corresponding hadronic form factors, and applies factorization to relate semi-leptonic and Class I non-leptonic decays. Such analyses [4, 5] which take, as input, quoted values [6, 7] for $\bar{B}^0 \rightarrow D^{**+} \ell^- \bar{\nu}_{\ell}$ conclude that production of narrow and broad D^{**} states are similar. Meanwhile, to reach this conclusion, they have to discard the measurement of $\bar{B}^0 \rightarrow D_0(2300)^+ \pi^-$ which implies, as a consequence of factorization, a very small value for the production of the $D_0(2300)$ meson in semi-leptonic decays, when compared with the rates measured for narrow states. This could seem to be justified because such a low value, evaluated for $\bar{B}^0 \rightarrow D_0(2300)^+ \ell^- \bar{\nu}_{\ell}$, appears to be in contradiction with the rates measured in experiments for this channel. However, on the opposite, we think that the non-leptonic data for the $D_{1/2}$ are much more trustable than the semi-leptonic ones. Indeed, the identification of the $D_0(2300)$ in the non-leptonic channel is supported by 1) the extraction of the D_V^* and 2) the measure of the phase shift, while no such work has been done in the semi-leptonic case (except, for the D_V^* , the work reported in [8]). Mo-

reover, from a theoretical point of view, the smallness of the transitions to the $D_{1/2}$ states with respect to the $D_{3/2}$ ones has been anticipated using, initially, quark models and, later on, by direct LQCD evaluations.

We have considered again this problem and propose a model, based also on the *LLSW* parameterization and which uses all the measured non-leptonic Class I decays in the framework of factorization. This model agrees with LQCD and relativistic quark models (RQM) expectations. Because, in this model, production of broad D^{**} mesons is expected to be much smaller than the production of narrow states, it is necessary to add another broad component to be able to explain the broad mass distributions measured in $\overline{B}^0 \rightarrow D^{(*)}\pi\ell^-\overline{\nu}_\ell$ decays. We find that $D_V^{(*)}$ decays can fill such a gap. In the following we detail our model and provide comparisons with the *LLSWBi* model in which the broad $D^{(*)}\pi$ mass distributions are explained by the contributions from D^{**} decays alone, as done in previous analyses and where the measurement from $\overline{B}^0 \rightarrow D_0(2300)^+\pi^-$ is not used.

Finally one is led to a solution with a $j = 1/2$ rate much smaller than the $j = 3/2$ one.

II. THEORETICAL INPUTS

We speak of "inputs" because one lacks a systematical theoretical treatment : rather, one is led to use a mixture of procedures, including the very experimental data which are to be explained, and fitting.

In addition, several ingredients a)b)c)d), as enumerated in the abstract, are available.

We can classify them also into two categories :

A. Dynamical results at $m_Q = \infty$

In the infinite quark mass limit, hadronic form factors that describe $\overline{B} \rightarrow D^{**}$, are determined by the two Isgur-Wise functions : $\tau_{3/2}(w)$ and $\tau_{1/2}(w)$. Their values at $w = 1$ and their w dependence are constrained by theory :

a) lattice QCD for $w = 1$ at $N_F = 0, 2$ [9] ; at $N_F = 2$:

$$\tau_{3/2} = 0.526 \pm 0.023, \tau_{1/2} = 0.296 \pm 0.026 \quad (1)$$

showing a striking difference between them, in contrast

with a naive non-relativistic (NR) expectation according to which these two quantities are equal.

These are trustable results which **cannot be disregarded**. In the most recent simulation the lattice spacing is reasonably small, $a = 0.085fm$, and the volume reasonably large : $24^3 \times 48$, although certain systematic errors are not estimated. Of course, they should be improved. One notes that, at $N_F = 2$, the inequality between $j = 1/2$ and $j = 3/2$ values is appreciably reinforced with respect to the older $N_F = 0$ ones.

b) quark models, which, although purely phenomenological, have the advantage of providing results for $w \neq 1$ as well.

Of course, there is a very large variety of quark models. We consider a class of models for current matrix elements where the calculation is decomposed into two steps : 1) the determination of the wave functions at rest and, 2) a procedure to derive from it the state in motion. Then there is first a variety of spectroscopic models, describing the spectrum and the wave functions at rest, i.e internal quark motion ; secondly, another variety comes from the way one describes the hadron motion.

As to spectroscopic models Among many, there is an outstanding one by Godfrey and Isgur (GI) [10], which we therefore decide to use. This model is unique in its covering of a very large number of hadronic states, both with light quarks and with heavy ones. One must underline that most predictions have been confirmed by later experiments. Although it is a complicated model with many parameters, these can be determined thanks to this covering of a very extended spectrum. This model has a relativistic kinetic energy and its success confirms the necessity of a relativistic treatment of quark internal motion inside hadrons, which is already implied by the fact that excitation energies are of the order of the reduced mass.

As to the description of hadron motion Here we shall use a specific framework, the one of Bakamjian and Thomas, to describe states in relativistic motion at $m_Q = \infty$. It has several advantages :

- α) it uses the standard three-dimensional wave functions at rest provided by spectroscopic models ;
- β) it is relativistic as to hadronic motion and even covariant ;
- γ) it satisfies the standard set of HQET sum rules, like Bjorken [11] and curvature [12] sum rules, Uraltsev sum rule [13]...

The last two points are important advantages as compared to non relativistic treatment of quark motion, even if we were adopting the GI spectroscopic model. Note that a NR treatment of hadron motion is not satisfactory for the full range of w since the 3-velocity at w_{max} is large even in the "Equal Velocity Frame" which minimizes velocities : $v = \sqrt{(w-1)/2} \simeq 0.4$.

Moreover these differences lead to quite different quantitative results. In the NR quark models with non-relativistic treatment of both internal quark velocities

and hadron motion, a general statement [?] would be :

$$\tau_{1/2}(w) = \tau_{3/2}(w) \quad (2)$$

in clear contradiction with the above lattice QCD results. The equality (2) assumes that there is no sizable spin-orbit force surviving at $m_Q = \infty$, which is not a theorem but seems reasonable from the spectroscopic models studies, whence identical rest frame wave functions.

In the BT framework, using the well known spectroscopic model of Godfrey and Isgur [10], one finds very different values for $j = 1/2$ and $j = 3/2$ [14] :

$$\tau_{3/2}(1) \simeq 0.5, \tau_{1/2}(1) \simeq 0.25 \quad (3)$$

in full agreement with QCD. This strikingly large difference is a general feature of the BT approach, which provides an intuitive explanation : it is due to the typically relativistic effect of Wigner rotations of spin, included in the BT approach, which acts differently on $j = 3/2$ and $j = 1/2$ states in motion and which is completely independent of the presence of possible spin-dependent forces in the potential. Note that, more generally, the inequality of the $\tau(1)$'s is suggested by the Uraltsev sum rule :

$$\Sigma_n \left(|\tau_{3/2}^{(n)}(1)|^2 - |\tau_{1/2}^{(n)}(1)|^2 \right) = 1/4 \quad (4)$$

which contradicts the equality (2) under the assumption of dominance of $n = 0$.

In summary, one should consider the marked difference between $\tau_{3/2}(1)$ and $\tau_{1/2}(1)$ as a solidly settled result (see the extensive discussions by Bigi et al.[15], see also [16] and the work on zero-recoil sum rules of [17] and [18]. In the latter reference the point of view of the authors on this matter is expressed at the end of subsection 6.3.2). Combined with the appropriate kinematical factors, and converted into branching ratios, this leads to the still more striking inequality :

$$\mathcal{B}(\overline{B}^0 \rightarrow D_{1/2}) \ll \mathcal{B}(\overline{B}^0 \rightarrow D_{3/2}) \quad (5)$$

by around one order of magnitude, and **we claim to provide a model which both satisfies this strong inequality and fits well the data.**

The quantitative agreement of the BT prediction with the lattice QCD one gives encouragement to trust the predicted shapes at $w \neq 1$, which are another crucial theoretical input.

The full shape is well approximated by a relativistic quark-model inspired description [20] :

$$\tau_{3/2(1/2)}(w) = \tau_{3/2(1/2)}(1) \times \left(\frac{2}{w+1} \right)^{2\sigma_{3/2(1/2)}} \quad (6)$$

Numerically :

$$\sigma_{3/2}^2 \simeq 1.5, \quad \sigma_{1/2}^2 \simeq 0.8 \quad (7)$$

These values are in contrast with what would be given in a fully NR treatment namely a common and much

lower value, of order 0.4 (obtained from [19] and skipping the relativisation factor κ .)

Other analyses use instead a linear approximation for the τ -functions : $\tau_i(w) = \tau_i(1) \times \left(1 - \sigma_{i,lin.}^2 (w-1) \right)$. It can be checked that $\sigma_{i,lin.}^2 = \sigma_i^2$ when $w = 1$. In practice the two descriptions are rather similar because the w variation range, between 1 and $w_{max} = (m_B^2 + m_{D^{**}}^2)/(2m_B m_{D^{**}})$ is limited anyway. Meanwhile, significant differences are expected, from the two parameterizations, when comparing semi-leptonic decays with a light or an heavy lepton, as evaluated in Table XIII.

Why start from $m_Q = \infty$?

The visible difficulty is that one has presently trustable quantitative statements only for $m_Q = \infty$. This derives from different reasons :

1) as to lattice QCD, it is the fact that it is very difficult to treat directly the finite masses m_b, m_c , all the more for transitions to excitations. Thus one has been led presently to use a $m_Q = \infty$ framework. Then, to treat finite $w \neq 1$, one would require infinite momenta, whence one is restricted to $w = 1$.

2) quark models have in general no such limitations. However the BT framework which we want to use is satisfactory only at $m_Q = \infty$. Indeed, it has been shown that the finite mass corrections cannot be trusted : they break covariance as well as certain important sum rules, in contrast with the $m_Q = \infty$ limit. One has not been able to cure this defect.

The consequence is that these dynamical results must be complemented by other statements, of a more general nature, which provide constraints on the physical transitions (of course at finite mass) or, equivalently, on finite mass corrections to the above dynamical results. Those questions are considered in points c) and d) below.

B. Use of general statements or relations

c) First of all, we rely on the validity of the factorization, as does in principle *LLSWB*. This phenomenon has been firmly established from the theoretical point of view (specially in the thorough demonstration and discussions by BBNS [21]). Moreover the order of magnitude of the departure from asymptotic BBNS factorization ($a_1 = 1 + \mathcal{O}(10\%)$) as observed from the phenomenological side, is such that it does not seem possible to doubt about this validity for the present decays. Of course, BBNS gives only an asymptotic statement, and a departure from this limit is quite expected (presence of various $1/m_Q$ corrections, m_c not very large, etc...). Factorization implies the well known Bjorken-Neubert relation [22] between the NL and SL decays at some q^2 (for

example m_π^2 for decay by pion emission), which is a very strong and useful constraint for the otherwise ill known SL differential q^2 distributions.

Practically, since we have no theoretical quantitative estimates of the departure of a_1 from the asymptotic BBNS result, we will apply factorisation in the following way. We fit $a_{1,eff.}$ in $\overline{B} \rightarrow D_{3/2}$ decays and find a value compatible with those obtained by analysing $\overline{B} \rightarrow D^{(*)}$ transitions (see Sec. VI). Then, in our final analysis, we impose a constraint in the fits : $a_{1,eff.} = 0.93 \pm 0.07$. This $a_{1,eff.}$ will also be used for cases where experimental data are lacking or not precise enough. This procedure is, in principle, valid for Class I decays with emission of a light meson. But we shall extend it to predict NL processes where a charmed strange meson is emitted like $\overline{B} \rightarrow D^{**}D_s^{(*)}$; although in such a case the asymptotic theorem of BBNS does not apply, it is a fact that, once more, one obtains a value of $a_{1,eff.}$ close to 1 from the measured processes.

d) HQET and $1/m_Q$ expansion,

Let us comment about d). The constraints from HQET expansion as performed in [3] and further work, including order $\mathcal{O}(1/m_Q)$ corrections, are crucial too as a necessary complement to the $m_Q = \infty$ predictions.

On the determination of the $\mathcal{O}(1/m_Q)$ subdominant functions.

One must stress that the constraints d) do not lead to quantitative statements on the finite mass corrections; they rather yield a parameterization of these finite corrections. They leave us with a large number of unknown parameters and functions of w . Some of those parameters, like $\overline{\Lambda}$, (quoted as Set 1 in the following) can be estimated otherwise, as explained in Section II C. One could think of fixing the remaining unknown ones (Set 2) by fits to the experimental data. But there remains at least a host of unknown functions of w . For instance, for $j = 3/2$, one needs in principle the ten functions : $\tau_1(w), \tau_2(w), \eta_{ke}^{b,c}(w), \eta_{1,2,3}^{b,c}(w)$ in *LLSW* notation[?], which is of course too much to be fitted at present. This number is reduced thanks to the fact that the η_i^b 's and η_{ke}^b are present only in one combination, $\eta^b = \eta_{ke}^b + 6\eta_1^b - 2\eta_2^b(w-1) + \eta_3^b$ but the problem remains.

Many further assumptions must then be added :

e) an additional but reasonable assumption of rough proportionality of the latter functions to the dominant Isgur-Wise functions reduces them to numerical parameters, denoted with "hats", but one remains however with a host of unknown numbers. For $D_{3/2}$ mesons, present data are sensitive to the values of $\hat{\eta}_{1,3}$ and $\hat{\tau}_1$, whose values we have determined, while some guesses have to be used to define a possible range of variation for the other two quantities : $\hat{\eta}_2$ and $\hat{\tau}_2$. For $D_{1/2}$ mesons, data are much less accurate and fits have the same sensitivity to $\hat{\chi}_{1,2}$ or $\hat{\chi}_1$ and one can obtain the value for only one of

these quantities. We choose, arbitrarily, to fit $\hat{\chi}_1$.

f) of course, one would like, however, to find some reasons for that selection, or to find consistency checks for the physical soundness of the values of the parameters found in this way.

-*LLSW* [1] proposed an additional expansion in $w-1$ (the latter too being small, of magnitude at most $\simeq 0.3 \simeq \epsilon_c = 1/2m_c$) in the narrow width approximation ($w_{max} \simeq 1.3, m_c \simeq 1.5 GeV$). Were this valid, it would allow to skip $\tau_{1,2}$ terms as being of higher order and to be left with the η 's. However, of course, this supposes that the $\tau_{1,2}$ are not large, a point for which there is no guarantee (in fact one often retains the reverse, i.e. dropping the η 's in favor of the $\tau_{1,2}$). In the present analysis we have not used any expansion in $w-1$ and we take the full $1/m_Q$ expansions of the Lorentz invariant form factors given in [3]. The validity of this framework requires that unknown quantities that enter in the expansion are of order $\overline{\Lambda}$. This is what we do verify for fitted quantities, therefore we have assumed that quantities, not determined by the fit, are also of that order to evaluate their contribution to systematic uncertainties.

-inspiration from quark models can help to check the soundness of fit results, at least qualitatively. As explained above, one cannot trust the BT approach for finite mass corrections, and this is the main obstacle to get physical results in this quark model approach. Then one may return to the NR model of center of mass motion, but only to get a qualitative understanding. An example is the η functions, which correspond in naive terms to the modification of the wave functions induced by the change of m_Q from ∞ to its real value in the Schrödinger equation.

Knowing theoretically the "true" (infinite mass) $\tau_{3/2}(w=1)$, the magnitude of the corrections at $w=1$ which appear in the combination $\frac{\eta^b}{2m_b} + \frac{\eta_{ke}^c}{2m_c}$ (corresponding to our $\hat{\epsilon}_{3/2}$ below), can be rather well determined with a stable value in the various fits to the data, and it is found to be neatly **negative**.

A fully NR calculation of the effect of $\mathcal{O}_{ke}(v=(1,0,0,0))$ (naively interpreted as the effect of the change of the kinetic energy on the wave functions in the rest frame) suggests a negative $\eta_{ke}^c(w=1)$ corresponding to the effect on the final state. η_{ke}^b on the contrary should be positive, but the combination η^b corresponds to the total effect on the state vectors, including $\mathcal{O}_{mag}(v=(1,0,0,0))$, and, naively interpreted, includes the large spin-spin force present at finite mass. In the GI model, it is found to be neatly negative by numerical calculation.

Then it is encouraging to find consistency between the theoretically expected sign and the finding of the fits. One could hope to estimate similarly the signs and order of magnitude of the remaining η_i^c 's, but this requires interpreting them separately in the quark model (see Appendix B).

g) on the whole, at present, there is no theoretical estimate for the values of the different parameters that enter in the *LLSW* expansion, except, perhaps, a qualitative

one of the η 's if one follows the arguments above (see also Appendix B).

C. Evaluation of HQET parameters

In the framework of HQET, masses of charm and beauty mesons are used to evaluate values of the parameters (named Set 1 in the following) that enter in some of the $1/m_Q$ corrections [3], the relation being :

$$m_{H_{\pm}} = m_Q + \bar{\Lambda}^H - \frac{\lambda_1^H}{2m_Q} \pm \frac{n_{\mp}\lambda_2^H}{2m_Q} + \dots \quad (8)$$

The total spin (J_{\pm}) of the resonance (H_{\pm}) is expressed in terms of the total spin (s_l) of the light hadronic system as : $J_{\pm} = s_l \pm 1/2$. while $n_{\pm} = 2J_{\pm} + 1$ is the number of spin states. Values of these different quantities and those of meson masses, adopted in our analysis, are indicated in Table I. We have not considered I-spin averaged masses and used only charged ($c\bar{d}$) states for charm and neutral states for beauty ($b\bar{d}$).

meson	J^P	s_l^{π}	n_{\pm}	charm mass	beauty mass
D^+/\bar{B}^0	0^-	$1/2^-$	$n_- = 1$	1869.65 ± 0.05	5279.65 ± 0.12
D^{*+}/\bar{B}^{*0}	1^-	$1/2^-$	$n_+ = 3$	2010.26 ± 0.05	5324.70 ± 0.21
D_1^+/\bar{B}_1^0	1^+	$3/2^+$	$n_- = 3$	2423.8 ± 1.1	5726.1 ± 1.4
D_2^{*+}/\bar{B}_2^{*0}	1^+	$3/2^+$	$n_+ = 5$	2465.4 ± 1.3	5739.5 ± 0.7
$D_0(2300)^+$	0^+	$1/2^+$	$n_- = 1$	2330 ± 20	(?)
$D_1(2430)^+$	1^+	$1/2^+$	$n_+ = 3$	$2452 \pm (?)$	(?)

TABLE I. The three doublets of heavy mesons having, respectively, a total spin and parity of their light component, s_l^{π} , equal to $1/2^-$, $3/2^+$ and $1/2^+$. The masses are given in MeV.

We use, for $\bar{\Lambda}^H$, the notations $\bar{\Lambda}$, $\bar{\Lambda}_{3/2}$ and $\bar{\Lambda}_{1/2}$ for the s_l^{π} doublets $1/2^-$, $3/2^+$ and $1/2^+$ respectively.

Considering only the first order expansion in $1/m_Q$ of Eq. (8), the ratio (r_Q) between charm and beauty quark masses is equal to :

$$r_Q = \frac{m_c}{m_b} = \frac{m_{B^*} - m_B}{m_{D^*} - m_D} = 0.3215 \pm 0.0015. \quad (9)$$

The difference between the $\bar{\Lambda}^H$ values for the three doublets can be expressed in terms of the ratio between heavy quark masses and of the values of spin averaged masses (\bar{m}) [3]. We have obtained :

$$\bar{\Lambda}_{3/2} - \bar{\Lambda} = (396.0 \pm 1.5) \text{ MeV}. \quad (10)$$

For the $1/2^+$ doublet the corresponding estimate is more uncertain because the associated B -meson states are still un-measured. From the masses of charm states we estimate : $\bar{\Lambda}_{1/2} - \bar{\Lambda} \sim 366 \text{ MeV}$.

These values for $\bar{\Lambda}_{3/2} - \bar{\Lambda}$ and $\bar{\Lambda}_{1/2} - \bar{\Lambda}$ agree with previous determinations.

To evaluate absolute values for heavy quark masses and $\bar{\Lambda}$ one needs a value for λ_1 . In previous analyses, the value $\lambda_1 = -0.2 \text{ GeV}^2$ was used; in a recent report from the HFLAV collaboration [6], the value $\lambda_1 = (-0.362 \pm 0.067) \text{ GeV}^2$ was obtained from an analysis of B -meson semi-leptonic decays. In Table II a summary is given for the values of the different parameters entering in the analysis (first line, with $\lambda_1 = -0.362 (\text{GeV})^2$).

λ_1	$\bar{\Lambda}$	$\bar{\Lambda}_{3/2}$	$\bar{\Lambda}_{1/2}$	m_c	m_b
-0.362	0.245	0.641	0.611	1.618	5.032
-0.2	0.4	0.8	0.76	1.4	4.8

TABLE II. Values of HQET parameters used in the evaluation of $1/m_Q$ corrections (first line). The last line gives the values used in previous analyses. The various quantities are expressed in GeV, except for $\lambda_1 (\text{GeV}^2)$

D. Evaluation of parameters entering in the LLSW parameterization

In the infinite quark mass limit, hadronic form factors that describe $\bar{B} \rightarrow D^{**}$, are determined by the two Isgur-Wise functions : $\tau_{3/2}(w)$ and $\tau_{1/2}(w)$ respectively, which have been introduced in Eq. (6). It has been noted [3] that one can define useful effective functions including finite mass corrections to replace the IW functions : namely, particularising at $w = 1$, one writes :

$$\tau_{3/2}^{eff.}(1) = \tau_{3/2}(1) + \frac{\eta_{ke}(1)}{2m_c} + \frac{\eta_b(1)}{2m_b} = \tau_{3/2}(1) \times |1 + \hat{\epsilon}_{3/2}| \quad (11)$$

$$\tau_{1/2}^{eff.}(1) = \tau_{1/2}(1) + \frac{\chi_{ke}(1)}{2m_c} + \frac{\chi_b(1)}{2m_b} = \tau_{1/2}(1) \times |1 + \hat{\epsilon}_{1/2}|$$

In Table III are reminded the parameters that enter in the expressions of Lorentz-invariant form factors for the LLSW parameterization of $\bar{B} \rightarrow D^{**}$ transitions.

III. $\bar{B}^0 \rightarrow D^{**}$ EXPERIMENTAL RESULTS USED AS CONSTRAINTS

Input data, in this analysis, are obtained by averaging branching fraction measurements of non-leptonic Class I, $\bar{B}^0 \rightarrow D^{**,+}\pi^- (K^-)$, and semi-leptonic decay $\bar{B} \rightarrow D^{**}\ell^-\bar{\nu}_{\ell}$ channels. These last values, obtained separately for charged and neutral B -mesons, are combined, assuming the equality of corresponding partial decay widths for charged and neutral B -mesons, and averaged values are expressed in terms of the \bar{B}^0 . We have taken into account possible correlations between the different

	parameters list	evaluation	constraints from theory
Set 1	$m_{b,c}, \bar{\Lambda}, \bar{\Lambda}_{3/2}, \bar{\Lambda}_{1/2}$	using HQET	see Section II C
Set 2 for $D_{3/2}$ mesons	$\tau_{3/2}(1)$	fitted	0.53 ± 0.03
	$\hat{\epsilon}_{3/2}$	fitted	
	$\sigma_{3/2}^2$	fitted	1.5 ± 0.5
	$\hat{\eta}_{1,3}, \hat{\tau}_1$	fitted	
	$\hat{\eta}_2, \hat{\tau}_2$	set to zero	$\pm 0.5 \text{ GeV}$ for syst.
Set 2 for $D_{1/2}$ mesons	$\tau_{1/2}^{eff.}(1)$	fitted	0.20 ± 0.06
	$\sigma_{1/2}^2$	fitted	$\sigma_{3/2}^2 - \sigma_{1/2}^2 = 0.7 \pm 0.5$
	$\hat{\chi}_1$	fitted	
	$\hat{\chi}_2, \hat{\zeta}_1$	set to zero	$\pm 0.5 \text{ GeV}$ for syst.

TABLE III. List of the parameters that enter in LLSW formalism. The two last columns indicate how values of these quantities are obtained in the present analysis. When no information is available on a parameter, it is set to zero and a range of $\pm 0.5 \text{ GeV} \sim \pm \bar{\Lambda}$ is used to evaluate a plausible contribution to systematic uncertainties.

decay channel	this analysis	analysis [4] (2016)	PDG(2020) or HFAG ⁽³⁾
$\mathcal{B}(\bar{B}^0 \rightarrow D_2^{*+} \pi^-) \times 10^4$	5.85 ± 0.42	5.9 ± 1.3	5.85 ± 0.43
$\mathcal{B}(\bar{B}^0 \rightarrow D_2^{*+} K^-) \times 10^5$	4.7 ± 0.8	not used	5.0 ± 0.9
$\mathcal{B}(\bar{B}^0 \rightarrow D_2^{*+} \ell^- \bar{\nu}_\ell) \times 10^3$	3.09 ± 0.32	2.8 ± 0.4	3.18 ± 0.26
$\mathcal{B}(\bar{B}^0 \rightarrow D_1^+ \pi^-) \times 10^4$	7.12 ± 1.13	7.5 ± 1.6	6.6 ± 2.0
$\mathcal{B}(\bar{B}^0 \rightarrow D_1^+ \ell^- \bar{\nu}_\ell) \times 10^3$	6.40 ± 0.44	6.2 ± 0.5	6.24 ± 0.54
$\mathcal{B}(\bar{B}^0 \rightarrow D_0(2300)^+ \pi^-) \times 10^4$	1.19 ± 0.12	not used	1.14 ± 0.12
$\mathcal{B}(\bar{B}^0 \rightarrow D_0(2300)^+ \ell^- \bar{\nu}_\ell) \times 10^3$	2.2 ± 1.2	4.1 ± 0.7	3.9 ± 0.7 ⁽⁴⁾
$\mathcal{B}(\bar{B}^0 \rightarrow D_1(2430)^+ \pi^-) \times 10^4$	0.21 ± 0.27 ⁽¹⁾	not used	not quoted
$\mathcal{B}(\bar{B}^0 \rightarrow D_1(2430)^+ \ell^- \bar{\nu}_\ell) \times 10^3$	1.4 ± 1.3	1.9 ± 0.5	1.8 ± 1.5 ⁽⁴⁾
$\mathcal{B}(\bar{B}^0 \rightarrow D_0(2300)^+ K^-) / \mathcal{B}(\bar{B}^0 \rightarrow D_2^{*+} K^-)$ ⁽²⁾	0.84 ± 0.36	not used	

TABLE IV. Measured branching fractions used as constraints in the present analysis. In the two last columns are indicated the values used in a previous analysis and those quoted in PDG [7] or obtained by HFAG [6]. As compared with our numbers, these values differ mainly in the estimate of the production of broad D^{**} states in B -meson semi-leptonic decays. Analysis [4] differs also by the fact that non-leptonic measurements of $D_{1/2}$ states are not included. ⁽¹⁾: we have not used the measured value for $\mathcal{B}(\bar{B}^0 \rightarrow D_1(2430)^+ \pi^-)$ [23] as constraint in our nominal fit because this is still a preliminary result and we have instead compared this value to our expectation. ⁽²⁾: $D^{**,+}$ mesons are reconstructed in the $D^0 \pi^+$ final state. ⁽³⁾: values from PDG and HFAG have been modified using results quoted in Table VI. ⁽⁴⁾: values from HFAG [6], the uncertainty on $\mathcal{B}(\bar{B}^0 \rightarrow D_1(2430)^+ \ell^- \bar{\nu}_\ell)$ is multiplied by a factor three to account for the poor compatibility between the three measurements used to obtain the average value.

Production of $D_{1/2}$ mesons in semi-leptonic decays, reported in the two last columns of Table IV, are derived from HFAG [6] whereas those used in our analysis are obtained using a different approach, as explained in Section III B. As illustrated from the values given in Table

uncertainties, corrected intermediate branching fractions [7], and used the hypotheses explained in Section III A to evaluate D^{**} absolute decay branching fractions. Values obtained in this way are compared with those used in a previous analysis [4] in Table IV. The first lines are relative to the production of narrow ($D_{3/2}$) states, then they correspond to broad ($D_{1/2}$) states and the last line reports a ratio between the production of narrow and broad states. Therefore, apart for the last constraint, it is possible to investigate the production of narrow and broad states, independently.

IV and from the results of the fits quoted in Tables XIII and XVIII, estimates for $D_1(2430)$ are not accurate, with about 100% uncertainty, once taking into account the fact that existing measurements are rather incompatible, with $\chi^2/NDF = 18/2$, and if we scale the uncertainty,

obtained on the average value, using the "PDG recipe" that corresponds to a factor three. Such a scaling factor is not included in the [4] analysis and the present value from PDG ($\sim (4 \pm 1) \times 10^{-3}$), not quoted in Table IV, is based on the measurement from BaBar alone, not including the other two results that enter in the HFAG average, and which are rather different, in particular the one from Belle which does not see a signal and quotes a stringent limit.

In addition, the Belle collaboration [8] has measured the semi-leptonic decay branching fraction $\overline{B}^0 \rightarrow D_2^{*+} \ell^- \bar{\nu}_\ell$ in four bins of the variable $w = v_D \cdot v_B = (m_B^2 + m_{D_2^*}^2 - q^2)/2m_B m_{D_2^*}$; $q^2 = m^2(\ell^- \bar{\nu}_\ell)$. The sum of these fractions is normalized to unity therefore, in the following, because we do not have the full error matrix on these measurements available, we use the first three results and assume that they are independent.

w bin	fraction (%)
[1.00, 1.08]	6.0 ± 2.3
[1.08, 1.16]	30.0 ± 5.4
[1.16, 1.24]	37.5 ± 6.2
[1.24, 1.32]	26.5 ± 6.2

TABLE V. Measured fractions of the $\overline{B}^0 \rightarrow D_2^{*+} \ell^- \bar{\nu}_\ell$ decay width in several w bins.

Values quoted in the third column of Table IV are used in Appendix C to demonstrate that our code is able to reproduce the values obtained in [4] when using similar input values and hypotheses. Those given in the last column allow to perform a comparison between experimental values retained in our analysis and those quoted in "official" compilations.

A. Evaluation of absolute $D^{**,+}$ decay branching fractions

At present, absolute D^{**} decay branching fractions are obtained using hypotheses on the contribution of the various decay channels. For the D_1 , it is assumed that it decays only into $D^* \pi$ and $D \pi \pi$ (through $D_0(2300) \pi$). The D_2^* is expected to decay only into $D \pi$ and $D^* \pi$. For broad states, we consider that the $D_0(2300)$ and the $D_1(2430)$ decay only into $D \pi$ and $D^* \pi$, respectively. Expected branching fractions are given in Table VI; they are similar to those used in [4].

B. Estimates for $\mathcal{B}(\overline{B}^0 \rightarrow D_{1/2}^+ \ell^- \bar{\nu}_\ell)$

Values for $D_0(2300)$ and $D_1(2430)$ production in \overline{B} hadron semi-leptonic decays, quoted in PDG or in HFAG, are obtained by fitting expected $D^{(*)} \pi$ mass distributions

$\mathcal{B}(D_2^* \rightarrow D \pi)$	0.61 ± 0.02
$\mathcal{B}(D_1^+ \rightarrow D^{*0} \pi^+)$	0.45 ± 0.03
$\mathcal{B}(D_1^+ \rightarrow D^+ \pi^+ \pi^-)$	0.15 ± 0.02
$\mathcal{B}(D_1(2430) \rightarrow D^* \pi)$	1
$\mathcal{B}(D_0(2300) \rightarrow D \pi)$	1

TABLE VI. Expected absolute D^{**} mesons decay branching fractions.

on measured $\overline{B} \rightarrow D^{(*)} \pi \ell^- \bar{\nu}_\ell$ events. This approach is reliable for $D_{3/2}$ mesons which appear as relatively narrow mass peaks. The determination of broad $D_{1/2}$ production is more difficult because one expects also contributions from $D_V^{(*)} \rightarrow D^{(*)} \pi$ and it is not clear how these components have been included in the analyses. For these reasons we have adopted another approach.

To evaluate $\mathcal{B}(\overline{B}^0 \rightarrow D_{1/2}^+ \ell^- \bar{\nu}_\ell)$ we use $\mathcal{B}(\overline{B} \rightarrow D^{(*)} \pi \ell^- \bar{\nu}_\ell)$ exclusive measurements from BaBar [24] and Belle [25], from which we subtract the expected contributions from $D_{3/2}$ and $D_V^{(*)}$ decays.

It has to be noted that, at present, in all these evaluations, contributions from higher mass resonances, which can decay into $D^{(*)} \pi$, are not specifically evaluated and therefore are fully or partially included in the rates estimated for $D_{1/2}$ mesons, depending on the approach.

$D_V^{(*)}$ components are normalized in an absolute way using values for $\mathcal{B}(\overline{B}^0 \rightarrow D^{(*)+} \ell^- \bar{\nu}_\ell)$ in which $D^{(*)}$ are on-mass shell, albeit with rather large uncertainties related to their mass dependence [2].

In the $D \pi$ channel, only the D_V^* component contributes. It is expected to decrease with the $D \pi$ mass value. For the D_V^{*0} channel, there is a natural threshold in the decay to $D^+ \pi^-$ because $m_{D^{*0}} < m_{D^+} + m_{\pi^-}$. For other charge combinations, the separation between so called D^* and D_V^* components is arbitrary, and therefore the absolute value of the D_V^* component depends on the considered threshold. In Belle, they use the following mass range $m_{D^{(*)} \pi} \in [2.05, 3] \text{ GeV}/c^2$ whereas, in BaBar they require $m_{D^0 \pi^+} - m_{D^0} > 0.18 \text{ GeV}/c^2$. These cuts are rather similar, being typically $40 \text{ MeV}/c^2$ above the nominal D^* mass.

To evaluate the uncertainty on these estimates we assume that the $D_V^{(*)}$ follows a relativistic Breit-Wigner mass distribution, modified by a Blatt-Weisskopf damping term with parameter $r_{BW} = 1.85 (\text{GeV}/c)^{-1}$ which is varied in the range $[1.0, 3.0] (\text{GeV}/c)^{-1}$.

1. $\mathcal{B}(\overline{B}^0 \rightarrow D_0(2300)^+ \ell^- \bar{\nu}_\ell)$

Averaging experimental measurements one obtains : $\mathcal{B}(\overline{B}^0 \rightarrow D \pi \ell^- \bar{\nu}_\ell) = (6.14 \pm 0.53) \times 10^{-3}$. We estimate the $D_V^* \rightarrow D \pi$ contribution, with $m_{D \pi} > 2.05 \text{ GeV}$, to be equal to : $(2.0 \pm 0.6) \times 10^{-3}$, in which the uncertainty

corresponds to the variation range used for r_{BW} . The D_2^* contribution is obtained from Tables IV and VI; it amounts to $(1.90 \pm 0.18) \times 10^{-3}$.

This gives :

$$\mathcal{B}(\overline{B}^0 \rightarrow D_0(2300)^+ \ell^- \bar{\nu}_\ell) = (2.2 \pm 1.2) \times 10^{-3} \quad (12)$$

as reported, after rounding, in Table IV. The uncertainty on the D_V^* estimate is added linearly to the total uncertainty evaluated for the other sources.

$$2. \quad \mathcal{B}(\overline{B}^0 \rightarrow D_1(2430)^+ \ell^- \bar{\nu}_\ell)$$

We use the same approach for the $D^*\pi$ hadronic final state. Averaging experimental measurements, one obtains : $\mathcal{B}(\overline{B}^0 \rightarrow D^*\pi\ell^- \bar{\nu}_\ell) = (8.39 \pm 0.54) \times 10^{-3}$. We estimate the D_V^{*+} contribution, using the coupling $g_{D^*D^*\pi} = \sqrt{2\frac{m_{D^*}}{m_D}} g_{D^*D\pi}$ which corresponds to a fictitious $\Gamma(D^* \rightarrow D^*\pi) = 2\Gamma(D^* \rightarrow D\pi)$, and we have added the expected (small) contribution from $D_V \rightarrow D^*\pi$. This gives : $(1.4 \pm 0.6) \times 10^{-3}$. D_V and D_V^* contributions are added incoherently because of helicity conservation and of the vanishing of $A - V$ interferences for the zero-helicity after the angular integration.

Subtracting the D_1^+ $((4.32 \pm 0.41) \times 10^{-3})$ and D_2^{*+} $((1.21 \pm 0.14) \times 10^{-3})$ contributions, obtained from Tables IV and VI, this gives :

$$\mathcal{B}(\overline{B}^0 \rightarrow D_1(2430)^+ \ell^- \bar{\nu}_\ell) = (1.4 \pm 1.3) \times 10^{-3} \quad (13)$$

as reported in Table IV. The uncertainty on the $D_V^{(*)}$ estimate is added linearly.

IV. PARAMETERIZATION OF SEMI-LEPTONIC AND NON-LEPTONIC DECAY WIDTHS

We indicate here the expressions we use to compute semi-leptonic and non-leptonic Class I decay branching fractions and explain how we have taken into account effects from contributions of virtual states.

A. Semi-leptonic transitions to real, discrete charmed states

Differential semi-leptonic $\overline{B} \rightarrow D_X \ell^- \bar{\nu}_\ell$ decay widths, with $D_X = D^{(*, **)}$, can be written as [4] :

$$\frac{d\Gamma}{dq^2} = C |\vec{p}| q^2 \left(1 - \frac{m_\ell^2}{q^2}\right)^2 \times \left[(H_+^2 + H_-^2 + H_0^2) \left(1 + \frac{m_\ell^2}{q^2}\right) + \frac{3m_\ell^2}{2q^2} H_t^2 \right] \quad (14)$$

with $C = G_F^2 |V_{cb}|^2 \eta_{EW}^2 / (96 \pi^3 m_B^2)$. \vec{p} is the three-momentum of the D_X in the B rest frame.

$$|\vec{p}| = m_{D_X} \sqrt{w_{D_X}^2 - 1} \quad (15)$$

in which $w_{D_X} = v_B \cdot v_{D_X}$ is the product of the 4-velocities of the two mesons.

$H_{\pm,0,t}$ are helicity form factors which are expressed in terms of, q^2 dependent, Lorentz invariant form factors ($FF(q^2)$) and depend on the considered meson D_X . Accurate parameterizations of $FF(q^2)$ are obtained for D (we use [26]) and D^* mesons (we use [27, 28]). For D^{**} mesons, expressions are taken from [3]. They correspond to expansions at first order in $1/m_{c,b}$ and α_s . For $D_{3/2}$ mesons, expressions that contain $1/m_{c,b} \times \alpha_s$ corrections are also available and have been included.

B. Semi-leptonic transitions to virtual charmed states

Let us now consider the physical case where the charmed state terminates on a two-body continuum like $D^{(*)}\pi$. As a useful intermediate step, one now considers fictitious weak transitions to intermediate virtual D^{**} or $D^{(*)}$, which represent the weak vertex part of the overall process, with the charmed leg bearing a momentum squared $p^2 = m^2 (= m_{D^{(*)}\pi}^2)$, different from the nominal squared mass of the state $m_{D_X}^2$ (of course, in the overall process, leading for instance to a $D\pi$ final state, one has to introduce a D^* propagator relating the weak vertex to the strong vertex which couples the virtual state to $D\pi$). If one considers production of virtual D^{**} mesons (that will get a Breit-Wigner distribution for m) or of virtual $D^{(*)}$, noted usually $D_V^{(*)}$, mesons, with m higher than their nominal mass value $m_{D^{(*)}}$, the invariant form factors at the weak vertex are expected to be also dependent on $m \neq m_{D_X}$.

However, in the absence of a theoretical knowledge of this dependence we assume simply :

$$FF(m, q^2) = FF(m_{D_X}, q^2) \quad (16)$$

in the expressions of helicity form factors, while keeping $m \neq m_{D_X}$ dependence of the kinetic quantities, such as momenta, in the additional factors entering in these expressions. This procedure is illustrated in the following example of the production of a virtual D_V meson of mass $m \neq m_D$. There are two invariant form factors noted : $f_{+,0}(m, q^2)$. Helicity form factors are expressed as :

$$\begin{aligned} q H_0 &= 2 m_B |\vec{p}| f_+(m_D, q^2) \\ q H_t &= (m_B^2 - m^2) f_0(m_D, q^2). \end{aligned} \quad (17)$$

The two other form factors, H_{\pm} , vanish because of helicity conservation. In these expressions and in Eq. (14), the decay momentum is evaluated at the virtual mass m : $|\vec{p}| = m \sqrt{w^2 - 1}$ with $w = (m_B^2 + m^2 - q^2) / (2 m m_B)$. Expressions relating helicity and invariant form factors

when a D^* meson is emitted can be found in [28] and in [4] in case of D^{**} mesons. Since these formula are devised for real, discrete charmed states, one must modify the factors affecting the form factors when considering virtual charmed states.

C. Non-leptonic decays

Thanks to factorization, non-leptonic Class I decay widths $\Gamma(\overline{B}^0 \rightarrow D_X^+ P^-)$ are related to corresponding differential semi-leptonic decay widths, through the $H_t^{D_X}$ helicity form factor :

$$\begin{aligned} \Gamma(\overline{B}^0 \rightarrow D_X^+ P^-) &= \frac{|a_{1,eff}^{D_X \pi}|^2 f_P^2 G_F^2 |V_{ij}|^2 |V_{cb}|^2 |\vec{p}|}{16\pi m_B^2} q^2 (H_t^{D_X})^2 \Big|_{w_P}. \end{aligned} \quad (18)$$

In this expression, $q^2 = m_P^2$, f_P is the leptonic decay constant of the emitted charged meson P , and V_{ij} is the corresponding CKM matrix element.

$$w_P = \frac{m_B^2 + m_{D_X}^2 - m_P^2}{2 m_B m_{D_X}}. \quad (19)$$

If the virtual "mass" m of the D_X meson doesn't have the nominal value m_{D_X} , we will still use values of invariant form factors evaluated at $q^2 = m_P^2$ as above while taking the running mass to compute the other terms that enter in $H_t^{D_X}$ and in \vec{p} .

We term the factor $a_{1,eff}^{D_X \pi}$ "effective" because the non-leptonic decay width, that enters in Eq. (18), corresponds to the sum of the Class I diagram amplitude and of subdominant terms which correspond to exchange or penguin mechanisms, while the remaining factors in the right hand are those provided by the analytic expression for a pure Class I process.

Expressions for $\overline{B}^0 \rightarrow D^{**+} P^-$ partial decay widths, with $P = \pi^-$ or D_s^- , and for $\overline{B}^0 \rightarrow D^{**+} D_s^-$ are given in Appendix A. Corresponding quantities, obtained in the infinite quark mass limit, for non-leptonic - $\Gamma(\overline{B}^0 \rightarrow D^{**} \pi^-)$ - and for the differential semi-leptonic - $d\Gamma(\overline{B}^0 \rightarrow D^{**+} \ell^- \bar{\nu}_\ell)/dw$ - can be found, for example, in [29].

D. Finite width effects

To include effects from the mass distribution of resonances we express the differential decay width for a process in which a D^{**} is reconstructed in a given final state (i) as [2] :

$$\frac{d\Gamma_i}{ds} = \frac{1}{\pi} \frac{\Gamma_0(s) \sqrt{s} \Gamma_{i,D^{**}}(s)}{(s - m_{D^{**}}^2)^2 + s \Gamma_{D^{**}}^2(s)}. \quad (20)$$

$\Gamma_0(s)$ is the decay width for the process computed in the hypothesis of a virtual D^{**} of mass equal to \sqrt{s} . $\Gamma_{i,D^{**}}(s)$ is the partial decay width for the D^{**} , of mass \sqrt{s} , reconstructed in the i observed channel. $\Gamma_{D^{**}}(s)$ is the total D^{**} decay width at the mass \sqrt{s} .

When the current mass (\sqrt{s}) is higher than the threshold for the i decay channel :

$$\Gamma_{i,D^{**}}(s) = \Gamma_{i,D^{**}}(m_{D^{**}}^2) \left(\frac{p_i}{p_i^0}\right)^{2L+1} \left(\frac{m_{D^{**}}}{\sqrt{s}}\right)^2 \left(\frac{F_{i,L}(p_i)}{F_{i,L}(p_i^0)}\right)^2. \quad (21)$$

p_i and p_i^0 are the break-up momenta for the D^{**} decaying into the i -channel at masses equal to \sqrt{s} and $m_{D^{**}}$, respectively. $F_{i,L}(p_i)$ is a Blatt-Weisskopf damping factor. For decay channels with a threshold above the resonance mass, p_i^0 becomes imaginary and $F_{i,L}(p_i^0)$ cannot be evaluated. In these conditions we take :

$$\Gamma_{i,D^{**}}(s) = \frac{g_i^2 p_i^{2L+1}}{24\pi s} F_i^2(p_i) \quad (22)$$

in which g_i is the coupling of the D^{**} to the i -channel. This expression is used, in the following, to evaluate contributions from virtual D or D^* mesons to $D^{(*)}\pi$ final states.

$\Gamma_{D^{**}}(s)$ is the sum of all partial decay widths $\Gamma_{i,D^{**}}(s)$, opened at the mass \sqrt{s} .

In non-leptonic decays, the expression in Eq. (20) is multiplied by another damping factor (noted usually $(F_{B,i}(p'_i)/F_{B,i}(p_i^0))^2$) to account for strong interaction effects due to the hadron emitted with the D^{**} . p'_i is the momentum of the B decay products, evaluated in the B rest-frame [?].

V. CONSTRAINTS USED IN OUR ANALYSIS

The measurements used in our analysis are listed in Table IV, second column.

As to the theoretical constraints, there are three of them (see Table III) :

1) factorization. The validity of the factorization is checked, using $D_{3/2}$ events (see Section VI), and then it is used as a constraint in the final fits with $a_{1,eff}^{D^{**}\pi} = 0.93 \pm 0.07$ for all D^{**} states.

2) at $w = 1$ we use the constraint : $\tau_{3/2}(1) = 0.53 \pm 0.03$ as expected from LQCD [9]. Because $\tau_{3/2}$ is defined in the infinite quark mass limit it is necessary to introduce mass corrections and one parameter characterizing them $\hat{\epsilon}_{3/2}$, (see Eq. (12)) which is a useful combination of the basic ones introduced by *LLSW*. $\hat{\epsilon}_{3/2}$ is fitted, as well as a part of the other parameters. The data on $D_{1/2}$ mesons are less accurate and it is not possible to fit $\hat{\epsilon}_{1/2}$.

3) at $w \neq 1$, LQCD does not provide any information on the variation with respect to w of the two IW functions for which we use quark models, namely the BT calculations explained in the second section. Unfortunately, quark models cannot provide errors. Therefore, to use them in a fit, we have considered a rather large range of values of the slopes around the predicted one.

A. Comparison with the analysis of [5].

To validate our code, we check that, using the same input data (given in the third column of Table IV) and the same hypotheses, we reproduce the results published in [5](see Appendix C).

VI. PRODUCTION OF $D_{3/2}$ MESONS : A CHECK OF FACTORIZATION

In a first step, the analysis is restricted to the production of $D_{3/2}$ mesons to quantify the importance of $1/m_Q$ corrections and to check the applicability of the factorization property. We have required that $\tau_{3/2}(1) = 0.53 \pm 0.03$

and fitted the $\hat{\epsilon}_{3/2}$ correction. This is essentially equivalent to fitting directly $\tau_{3/2}^{eff}$. No constraint is used on $a_{1,eff}^{D_{3/2}\pi}$ and $\sigma_{3/2}^2$.

Data are first analyzed without any $1/m_Q$ correction. The fit probability is below 10^{-13} . This is mainly due to the fact that, in the infinite quark mass limit, theory predicts a production higher for the D_2^* as compared to the D_1 whereas it is measured two times lower.

Adding the Set 1 of $1/m_Q$ corrections improves the situation but the fit probability is still below 10^{-4} .

Therefore it is necessary to fit additional parameters which control the other $1/m_Q$ corrections. Fitting successively one among all other parameters, we end up with the results given in Table VII. All fit probabilities are higher than 10%.

X param.	$a_{1,eff}^{D_{3/2}\pi}$	$\sigma_{3/2}^2$	$\hat{\epsilon}_{3/2}$	X (GeV)	χ^2/NDF
$\hat{\eta}_1$	0.90 ± 0.05	-0.4 ± 0.7	-0.50 ± 0.09	-0.40 ± 0.11	3.4/4
$\hat{\eta}_3$	0.82 ± 0.05	-2.1 ± 0.7	-0.77 ± 0.07	3.2 ± 1.1	7.0/4
$\hat{\tau}_1$	0.81 ± 0.07	1.0 ± 0.7	-0.34 ± 0.12	0.75 ± 0.24	6.4/4
$\hat{\tau}_2$	0.89 ± 0.06	2.1 ± 0.5	-0.19 ± 0.11	2.9 ± 0.8	2.5/4
$\hat{\eta}_2$	0.86 ± 0.06	1.2 ± 0.6	-0.30 ± 0.11	-1.63 ± 0.44	3.8/4

TABLE VII. Results obtained using the constraint from theory on $\tau_{3/2}(1)$. Set 1 $1/m_Q$ corrections are used and one additional parameter from Set 2 is fitted, in addition to $\hat{\epsilon}_{3/2}$.

It can be noted that, depending on the choice of the additional fitted parameter, values of the slope ($\sigma_{3/2}^2$) and of the correction ($\hat{\epsilon}_{3/2}$) to the normalization of the IW function fluctuate. This comes from the fact that fitted individual parameters are also changing the w dependence of form factors and there are not enough measurements of the differential decay branching fractions versus w to constrain these variations. It results that fitted values for the IW slope can be highly correlated with the

value fitted for some of the additional parameters. In the following we therefore use the constraint expected from QM : $\sigma_{3/2}^2 = 1.5 \pm 0.5$ so that the w -dependence of the IW function verifies expectations from theory while we have no constraints on the precise values of all parameters entering in $1/m_Q$ corrections. One has to check, a posteriori, that such quantities are not too large so that the model we are using remains valid.

Results obtained for all possible fitted pairs of parameters are given in Table VIII. The fitted correction $\hat{\epsilon}_{3/2}$ is now rather independent on the choice of the fitted pair.

The value of $a_{1,eff}^{D_{3/2}\pi}$, fitted in each model, (see Tables VII and VIII), varies between 0.81 and 1.06 with uncertainties between 0.05 and 0.11. This is compatible with estimates of $a_{1,eff}^{D\pi} = 0.880 \pm 0.024$ and $a_{1,eff}^{D^*\pi} = 0.981 \pm 0.025$ we obtain by analysing corresponding decay channels. These values differ somewhat from the one

given by BBNS, but this is not unexpected since we are far from the asymptotic situation considered by those authors.

Therefore, in our final results we add, as a constraint, that $a_{1,eff}^{D^*\pi} = 0.93 \pm 0.07$ obtained from the measurements when either a D or a D^* is produced. This constraint is important, when evaluating systematic un-

X-Y param.	$a_{1,eff.}^{D_{3/2}\pi}$	$\sigma_{3/2}^2$	$\hat{\epsilon}_{3/2}$	X (GeV)	Y (GeV)	χ^2/NDF
$\hat{\eta}_1 - \hat{\eta}_3$	1.06 ± 0.08	1.45 ± 0.45	-0.19 ± 0.11	-0.45 ± 0.08	-0.78 ± 0.25	1.4/4
$\hat{\eta}_1 - \hat{\tau}_1$	0.83 ± 0.11	1.34 ± 0.57	-0.28 ± 0.10	0.05 ± 0.26	0.68 ± 0.73	6.7/4
$\hat{\eta}_1 - \hat{\tau}_2$	0.88 ± 0.06	1.55 ± 0.50	-0.27 ± 0.09	-0.07 ± 0.10	2.34 ± 1.24	2.7/4
$\hat{\eta}_1 - \hat{\eta}_2$	0.86 ± 0.06	1.55 ± 0.50	-0.24 ± 0.10	0.09 ± 0.17	-2.1 ± 1.1	3.7/4
$\hat{\eta}_3 - \hat{\tau}_1$	0.82 ± 0.05	1.75 ± 0.50	-0.18 ± 0.12	-0.52 ± 0.33	1.04 ± 0.31	4.6/4
$\hat{\eta}_3 - \hat{\tau}_2$	0.86 ± 0.05	1.66 ± 0.50	-0.27 ± 0.11	0.10 ± 0.23	2.9 ± 0.9	3.0/4
$\hat{\eta}_3 - \hat{\eta}_2$	0.89 ± 0.05	1.67 ± 0.48	-0.19 ± 0.11	-0.30 ± 0.26	-2.0 ± 0.5	2.8/4
$\hat{\tau}_1 - \hat{\tau}_2$	0.86 ± 0.06	1.75 ± 0.46	-0.25 ± 0.09	0.07 ± 0.33	2.8 ± 1.5	3.2/4
$\hat{\tau}_1 - \hat{\eta}_2$	0.98 ± 0.10	1.60 ± 0.41	-0.20 ± 0.10	-1.1 ± 0.7	-3.9 ± 1.6	1.9/4
$\hat{\tau}_2 - \hat{\eta}_2$	0.87 ± 0.05	1.65 ± 0.48	-0.25 ± 0.09	2.1 ± 2.2	-0.5 ± 1.1	3.0/4

TABLE VIII. Results obtained using the two constraints from theory on $\tau_{3/2}(1)$ and $\sigma_{3/2}^2$. Set 1 $1/m_Q$ corrections are used and two additional parameters from set 2 are fitted, in addition to $\hat{\epsilon}_{3/2}$.

certainties, to avoid that effects of a variation of a given parameter induce a large variation on a_1 and therefore correspond to effects that are outside the fact that the present analysis is done in the framework of factorization. This constraint is softer than the one used for this same property in previous analyses of these channels.

A. Fitted model parameters for $D_{3/2}$ production

As observed in Tables VII and VIII, the χ^2 obtained when fitting present data is mainly sensitive to the parameters $\hat{\eta}_1$, $\hat{\eta}_3$, and $\hat{\tau}_1$. There are enough measurements and constraints to determine these quantities with some accuracy. Values of the two other parameters, $\hat{\tau}_2$ and $\hat{\eta}_2$ cannot be determined from present data. We have evaluated effects from this indetermination by changing the values of these two quantities by $\pm 0.5 \text{ GeV}$ and by redoing the fit of the other parameters. The variation range we consider is obtained by noting that these quantities can have, at most, values similar to $\bar{\Lambda}$ so that the model remains valid.

B. Summary on $D_{3/2}$ production

In summary, production of $D_{3/2}$ in non-leptonic Class I B -meson decays is compatible with factorization.

The analysis can be done using the value expected from LQCD for $\tau_{3/2}(1) = 0.53 \pm 0.03$ but this differs from the $\tau_{3/2}^{eff.}(1)$ introduced in equation (12) by the quantity $\hat{\epsilon}_{3/2} = -0.2 \pm 0.1$, whose value has been fitted. We have verified, in Appendix B, that the minus sign of this correction agrees with theory. Combining these values we obtain :

$$\tau_{3/2}^{eff.}(1) = 0.42 \pm 0.06, \quad (23)$$

in agreement with previous analyses.

To have reasonable agreement between data and expectations we find that it is necessary to fit at least one, among the five parameters that control $1/m_Q$ corrections. In this case there remain four parameters that are unknown and it is difficult to obtain model uncertainties. Hopefully, present measurements and constraints from theory allow us to evaluate values of the three most important parameters that control the model. In this way we estimate to have a better control of systematic uncertainties that come from estimates of the values of quantities that are not fitted on data. We obtain :

$$\begin{aligned} \hat{\eta}_1 \text{ (GeV)} &= -0.32 \pm 0.13 \pm 0.03 \\ \hat{\eta}_3 \text{ (GeV)} &= -0.77 \pm 0.28 \pm 0.21 \\ \hat{\tau}_1 \text{ (GeV)} &= 0.36 \pm 0.35 \pm 0.35. \end{aligned} \quad (24)$$

in which the second uncertainty corresponds to the largest variations induced by changing the values of $\hat{\tau}_2$ and $\hat{\eta}_2$ by $\pm 0.5 \text{ GeV}$. We consider that this model uncertainty has to be added linearly to the one coming from the fit because we cannot favour any value for $\hat{\tau}_2$ and $\hat{\eta}_2$, within their considered variation range.

One cannot directly compare values obtained for $\hat{\eta}_{1,3}$ and $\hat{\tau}_1$ with previous determinations in which one or at most two of these parameters have been fitted on data. It can be noted that fitted values do not preclude the assumed validity of the $1/m_Q$ expansion because these quantities are of order $\bar{\Lambda}$. In Table IX we compare expected values for the ratios $\mathcal{R}_{D_{3/2}} = \mathcal{B}(\bar{B}^0 \rightarrow D_{3/2}^+ \tau^- \bar{\nu}_\tau) / \mathcal{B}(\bar{B}^0 \rightarrow D_{3/2}^+ \ell^- \bar{\nu}_\ell)$ with previous determinations.

$\mathcal{R}_{D_{3/2}}$ (%)	our analysis	[4](2016)	[5](2017)
$\mathcal{R}_{D_2^*}$	$6.1 \pm 0.5 \pm 0.2$	7 ± 1	7 ± 1
\mathcal{R}_{D_1}	$9.9 \pm 0.7 \pm 0.1$	10 ± 1	10 ± 2

TABLE IX. Comparison between expected values for $\mathcal{R}_{D_{3/2}}$.

VII. PRODUCTION OF $D_{1/2}$ MESONS :

$$\tau_{1/2}^{eff.}(1) \ll \tau_{3/2}^{eff.}(1)$$

Data on B -meson semi-leptonic decays into $D_{1/2}$ states are rather uncertain. In agreement with previous analyses (see Table XVII in Appendix C), we find that present data do not allow to determine the slope $\sigma_{1/2}^2$ of the corresponding IW function. In addition, the effect of $1/m_Q$ parameters is to modify the observed w dependence of form factors, therefore it is important, as explained in the previous section, to ensure that the variation of the IW function remains physical. Following relativistic quark model (RQM) expectations, we use $\sigma_{1/2}^2 = 0.8$ with a conventional error ± 0.5 .

For the same reasons it is not possible to fit the parameter $\hat{\epsilon}_{1/2}$.

Using measurements, relative to $D_{1/2}$ production in Table IV, apart for $\mathcal{B}(\bar{B}^0 \rightarrow D_1(2430)^+\pi^-)$ which is not published, and factorization with $a_1 = 1$, we have fitted $\tau_{1/2}^{eff.}(1)$ (see Table X).

Without fitting any additional $1/m_Q$ parameter, we obtain :

$$\tau_{1/2}^{eff.}(1) = 0.147 \pm 0.025, \quad (25)$$

with a 24% fit probability. This value is much smaller than $\tau_{3/2}^{eff.}(1)$ given in Eq. (23), in agreement with the theoretical expectations and in contradiction with *LLSWB*.

Let us now take into account the $1/m_Q$ corrections. The $\hat{\chi}_{1,2}$ and $\hat{\zeta}_1$ correction parameters provide enough flexibility in decay rate expressions to accommodate essentially any measured values, with an acceptable χ^2 probability. It is therefore needed to use additional constraints from theory.

LQCD expectation gives $\tau_{1/2}(1) = 0.296 \pm 0.026$. We have no predicted value for the quantity $\hat{\epsilon}_{1/2}$ which corresponds to $1/m_Q$ corrections on $\tau_{1/2}(1)$. If we assume that $\hat{\epsilon}_{1/2} = \hat{\epsilon}_{3/2}$, we expect $\tau_{1/2}^{eff.}(1) = 0.24 \pm 0.02$, which is higher than the measurement in Eq. (25). This can be due to either the fact that $\hat{\epsilon}_{1/2}$ differs from $\hat{\epsilon}_{3/2}$ or that other $1/m_Q$ corrections, not considered for the evaluation in Eq. (25) can have some effect. For these reasons, in the following, we use, as a constraint, the value : $\tau_{1/2}^{eff.}(1) = 0.20 \pm 0.06$ where the uncertainty is large enough to cover the two previous estimates.

Using these two constraints (on $\tau_{1/2}^{eff.}(1)$ and $\sigma_{1/2}^2$), and fitting one additional parameter, we obtain the values given in Table X.

Fit probabilities are close to 30% and values for the different parameters are reasonable, of the order of $\bar{\Lambda}$, but comparing with $D_{3/2}$ production one cannot identify a parameter to which the analysis is most sensitive and we are not able to fit more than one of these quantities, with reasonable accuracy, using present data. In the following

X param.	$\tau_{1/2}^{eff.}(1)$	$\sigma_{1/2}^2$	X	χ^2/NDF
no X	0.155 ± 0.025	1.0 ± 0.5	no value	3.5/3
χ_1	0.21 ± 0.06	0.80 ± 0.50	-0.27 ± 0.22	2.6/2
χ_2	0.21 ± 0.06	0.78 ± 0.50	0.37 ± 0.27	2.5/2
ζ_1	0.22 ± 0.06	0.76 ± 0.50	0.75 ± 0.44	2.3/2

TABLE X. Fitted values of one of the parameters entering in $1/m_Q$ corrections. $\tau_{1/2}^{eff.}(1)$ and $\sigma_{1/2}^2$ are constrained as explained in the text.

we adjust $\hat{\chi}_1$ and evaluate model systematic uncertainties changing $\hat{\chi}_2$ and $\hat{\zeta}_1$ by $\pm 0.5 GeV$.

VIII. PRODUCTION OF $D_{3/2}$ AND $D_{1/2}$ MESONS : COMBINED ANALYSIS AND SYSTEMATIC UNCERTAINTIES

We include in the analysis the data given in Table IV excluding the unpublished measurement of $\mathcal{B}(\bar{B}^0 \rightarrow D_1(2430)^+\pi^-)$. Constraints from theory on the parameters of the IW functions and the list of fitted quantities are given in Table III, Section IID.

The analysis is done taking into account the validity of factorization. for all D^{**} -meson production and using : $a_{1,eff.}^{D^{**}\pi} = 0.93 \pm 0.07$, see Section VI.

The ratio $\chi^2/NDF = 6.3/7$ corresponds to a fit probability of 51%.

Values of fitted parameters, given in Table XI, are almost identical with those obtained when considering separate productions of $D_{3/2}$ and $D_{1/2}$ mesons (see Sections VIB and VII).

$a_{1,eff.}^{D^{**}\pi}$	$\tau_{3/2}(1)$	$\sigma_{3/2}^2$	$\tau_{1/2}^{eff.}(1)$	$\sigma_{1/2}^2$
0.944 ± 0.062	0.53 ± 0.03	1.50 ± 0.50	0.21 ± 0.06	0.80 ± 0.70
$\hat{\epsilon}_{3/2}$	$\hat{\eta}_1 (GeV)$	$\hat{\eta}_3 (GeV)$	$\hat{\tau}_1 (GeV)$	$\hat{\chi}_1 (GeV)$
-0.18 ± 0.11	-0.32 ± 0.13	-0.77 ± 0.28	0.36 ± 0.35	-0.24 ± 0.26

TABLE XI. Fitted values of the reference model parameters, for $B \rightarrow D^{**}$ Lorentz invariant form factors. The first line contains parameters that are constrained by theory or from external measurements ($a_{1,eff.}^{D^{**}\pi}$). Quoted uncertainties are obtained from the fit.

Fitted quantities allow to obtain values for different branching fractions of a \bar{B}^0 meson decaying into $D^{**}\ell^-\bar{\nu}_\ell$, with a light or the τ lepton, as well as for non-leptonic decays. We have also considered $\bar{B}^0 \rightarrow D^{**,+}D_s^{(*),-}$ decays, in the framework of factorization.

To evaluate systematic uncertainties, values of not-fitted parameters are changed to $\pm 0.5 GeV$ and the largest variation on a fitted or derived quantity, that depends on fitted values, is used as systematic model uncertainty. For some of these quantities, mainly related

to the production of $D_{1/2}$ mesons, these variations are asymmetric, when compared to the value obtained with the reference model (in which the non-fitted parameters are set to zero). In this case we have symmetrized systematic uncertainties and corrected central values accordingly. Model uncertainties are added linearly to those from the fit because there is no reason to prefer a value for unfitted quantities, within their variation range.

Other sources of systematic uncertainties are considered as :

- effects from uncertainties on HQET parameters (Set 1). They are illustrated by using the values adopted in previous analyses (see Table II) ;
- effects of using a linear parameterization for the IW functions, versus w , in place of the dipole distribution (Eq. (6)) ;
- the effect of changing the parameterization of Blatt-Weisskopf terms in non-leptonic decays when the momentum of the emitted hadron is computed in the frame of the resonance in place of the B -meson rest frame (the former has been used by some experimental collaborations).

These observed variations are only indicative and can-

not be considered as really representative of corresponding systematic uncertainties values. In most cases, these sources are less important than uncertainties from the fit or from the model.

When evaluating a ratio between two derived quantities, correlations between the different uncertainties are taken into account.

In the following we detail our expectations and give comparisons with those obtained in another analysis, quoted as *LLSWBi*, which is close to those done in previous publications [4, 5]. Differences relative to our approach are listed in Appendix D. Numerical values, obtained in this way, are quoted also in appendices whereas corresponding expected distributions are compared with our results on the different Figures that follow.

A. Comparison between our model and the *LLSWBi* analysis for $D_{1/2}$ production in non-leptonic Class I decays

In Table XII we illustrate the differences between our model and the *LLSWBi* analysis for Class I non-leptonic decays.

channel	measured	our model	<i>LLSWBi</i> model
$\mathcal{B}(\overline{B}^0 \rightarrow D_0(2300)^+ \pi^-) \times 10^4$	1.19 ± 0.12	1.21 ± 0.12	10.0 ± 2.5
$\mathcal{B}(\overline{B}^0 \rightarrow D_1(2430)^+ \pi^-) \times 10^4$	0.21 ± 0.27	0.7 ± 0.7	3.2 ± 2.8
$\mathcal{R}_{\mathcal{K}}(D_0(2300), D_2^*)$	0.84 ± 0.36	0.35 ± 0.04	2.8 ± 0.7

TABLE XII. Comparison between measured and expected values for non-leptonic $\overline{B}^0 \rightarrow D_{1/2}$ transitions. $\mathcal{R}_{\mathcal{K}}(D_0(2300), D_2^*)$ is the ratio between the branching fractions $\mathcal{B}(\overline{B}^0 \rightarrow D_0(2300)^+ K^-)$ and $\mathcal{B}(\overline{B}^0 \rightarrow D_2^{*+} K^-)$, with the two D^{**} mesons decaying into $D^0 \pi^+$.

The measured values for $\mathcal{B}(\overline{B}^0 \rightarrow D_0(2300)^+ \pi^-)$ and $\mathcal{R}(D_0(2300), D_2^*)$ enter our model through the use of factorization. Therefore it is a check of consistency that the corresponding fitted values are in agreement with the data, as well as with theory, which predicts indeed that $j = 1/2$ transitions should be much smaller than $j = 3/2$ ones.

On the other hand, one can see that predictions of *LLSWBi* are in disagreement with the data by more than four standard deviations and too large by around one order of magnitude, which leads to discard the model. Keeping this in mind, it may nevertheless be useful to apply the same model to semi-leptonic decays for the sake of comparison with our own results, especially since *LLSW* is used by experimentalists in the analyses of the background to decays such as $\overline{B} \rightarrow D^* \ell \overline{\nu}_\ell$.

IX. D^{**} MESON PRODUCTION IN \overline{B}^0 SEMI-LEPTONIC DECAYS

Our results on decay branching fractions of \overline{B}^0 mesons into the four D^{**+} mesons are explained. In Sections IX B and IX C, expected hadronic mass and q^2 distributions are obtained for the $D^* \pi$ and $D \pi$ hadronic final states, respectively. Spectra are compared with the *LLSWBi* analysis and, to ease the comparison, total decay rates, expected in the two cases, have been scaled (only for plotting purposes) to the central values measured for the considered final states. Corresponding uncertainties are scaled also to agree with those obtained on measurements for $\mathcal{B}(\overline{B}^0 \rightarrow D^{(*)+} \pi^- \ell^- \overline{\nu}_\ell)$, with light leptons. Additional uncertainties, from the fit and the model, which appear when considering decays with a τ lepton or a D_s^- meson, are included.

A. Expected values for $\mathcal{B}(\overline{B}^0 \rightarrow D_i^{+} \ell^- \bar{\nu}_\ell)$ and corresponding q^2 distributions.**

Expected q^2 distributions in \overline{B}^0 semi-leptonic decays with a light or a τ lepton are given in Figures 1, 2, 3, and 4 for D_2^{*+} , D_1^+ , $D_0(2300)^+$, and $D_1(2430)^+$, respectively. Hatched areas correspond to uncertainties from the fit. Curves indicated with dots are the expected systematic uncertainties from the un-measured $\hat{\eta}_2$ and $\hat{\tau}_2$ parameters. Those indicated with triangles are from the un-measured $\hat{\chi}_2$ and $\hat{\zeta}_1$ parameters. In each figure the left plot is for light leptons and the right one for the τ .

Expected values for semi-leptonic branching fractions, with a light and the τ lepton, are given in Table XIII. Those obtained in the *LLSWBi* analysis are given in Appendix D1. To evaluate uncertainties on quoted values we have added linearly uncertainties from the fit and from the model. Values for other possible sources of uncertainties, quoted in Table XIII are simply indicative and usually are not dominant when compared with the others. It can be noted that ratios of branching fractions with a τ or a light lepton have a better accuracy because of correlations between the different uncertainties.

channel	value \pm fit	model	HQET	IW linear	Blatt-W.
$\mathcal{B}(\overline{B}^0 \rightarrow D_2^{*+} \ell^- \bar{\nu}_\ell) \times 10^3$	3.15 ± 0.30	0.	0.	0.01	0.02
$\mathcal{B}(\overline{B}^0 \rightarrow D_2^{*+} \tau^- \bar{\nu}_\tau) \times 10^4$	1.90 ± 0.29	0.05	0.	0.09	0.03
$\mathcal{R}_{D_2^*} \times 10^2$	6.03 ± 0.52	0.15	0.02	0.24	0.06
$\mathcal{B}(\overline{B}^0 \rightarrow D_1^+ \ell^- \bar{\nu}_\ell) \times 10^3$	6.40 ± 0.44	0.	0.	0.	0.
$\mathcal{B}(\overline{B}^0 \rightarrow D_1^+ \tau^- \bar{\nu}_\tau) \times 10^4$	6.30 ± 0.59	0.10	0.30	0.70	0.07
$\mathcal{R}_{D_1} \times 10^2$	9.84 ± 0.68	0.15	0.47	1.10	0.11
$\mathcal{B}(\overline{B}^0 \rightarrow D_0(2300)^+ \ell^- \bar{\nu}_\ell) \times 10^4$	5.1 ± 1.2	1.2	-0.2	0.4	-0.1
$\mathcal{B}(\overline{B}^0 \rightarrow D_0(2300)^+ \tau^- \bar{\nu}_\tau) \times 10^5$	5.0 ± 1.3	1.7	-0.1	0.6	0.1
$\mathcal{R}_{D_0(2300)} \times 10^2$	9.9 ± 1.5	1.0	0.4	0.4	0.1
$\mathcal{B}(\overline{B}^0 \rightarrow D_1(2430)^+ \ell^- \bar{\nu}_\ell) \times 10^4$	4.6 ± 3.7	0.9	0.3	-0.5	0.
$\mathcal{B}(\overline{B}^0 \rightarrow D_1(2430)^+ \tau^- \bar{\nu}_\tau) \times 10^5$	3.4 ± 2.7	0.6	0.3	-0.3	0.
$\mathcal{R}_{D_1(2430)} \times 10^2$	7.4 ± 1.2	1.6	0.1	0.4	0.1

TABLE XIII. Our expectations for semi-leptonic branching fractions with a light or a τ lepton and their ratio for individual D^{**} -meson states.

1. $D_{3/2}$ production

Values for semi-leptonic branching fractions with a light lepton and a $D_{3/2}$ meson are essentially identical with input measurements. This is because one has basically no measurement of the q^2 dependence of the different decay rates and because the normalisation is fitted through the $\tau_{3/2}$ and $\hat{\epsilon}_{3/2}$ parameters. Expected uncertainties on the production of D_1 and D_2^* , with a τ lepton are of about 20%. It can be noted that, in D_1 production, uncertainties on Set 1 (HQET) parameters and on the w expected dependence of $\tau_{3/2}$ may be not negligible. This is expected because HQET Set 1 corrections change the computed branching fraction with a D_1 by a large factor, as compared with the infinite quark mass limit prediction.

2. $D_{1/2}$ production

The value expected for $\mathcal{B}(\overline{B}^0 \rightarrow D_0(2300)^+ \ell^- \bar{\nu}_\ell) = (5.1 \pm 2.4) \times 10^{-4}$ is much smaller than the one usually anticipated from *LLSWBi*: $(39.1 \pm 7.2) \times 10^{-4}$, as given in Appendix D1. This result is a direct consequence of the use of factorization. Values expected for $D_1(2430)$ are similar but being affected by larger uncertainties one cannot draw any conclusion. Production of $D_{1/2}$ mesons in B -meson semi-leptonic decays is expected to be an order of magnitude smaller than the one of narrow states. In the production of $D_{1/2}$ mesons, model uncertainties are dominant when compared with the other considered sources of systematic uncertainties.

Expected branching fractions for $D_0(2300)$ and $D_1(2430)$ production have about 50% and 100% uncertainty, respectively. These relative uncertainties are even larger when a τ lepton is emitted.

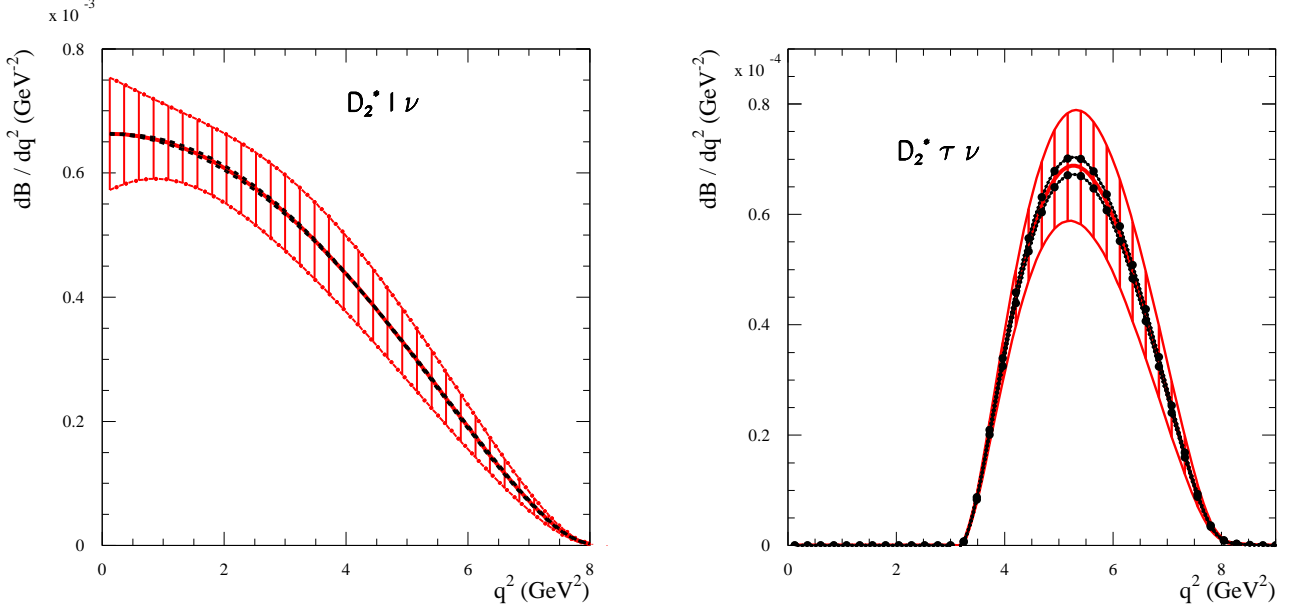


FIGURE 1. Expected q^2 distributions for $\overline{B}^0 \rightarrow D_2^{*+}$ in semi-leptonic decays. Hatched areas correspond to uncertainties from the fit, curves with dots indicate the model uncertainty. Other systematic uncertainties, indicated in Table XIII, are not displayed.

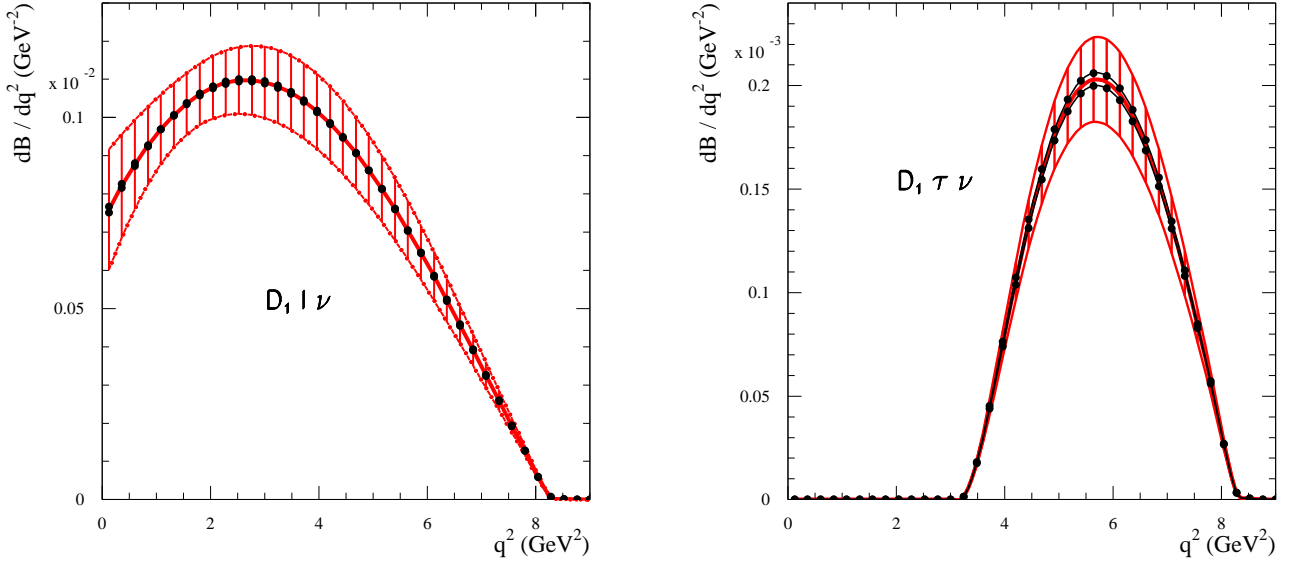


FIGURE 2. Expected q^2 distributions for $\overline{B}^0 \rightarrow D_1^+$ in semi-leptonic decays. Same conventions are used as in Fig.1.

3. Conclusions

In our analysis, the expected low production rates of broad, relative to narrow, D^{**} mesons comes from theo-

retical arguments and is in agreement with the factorization property. This low value implies that it has to be complemented by another source of events, to explain the measured broad mass distributions in $D^{(*)}\pi$ hadro-

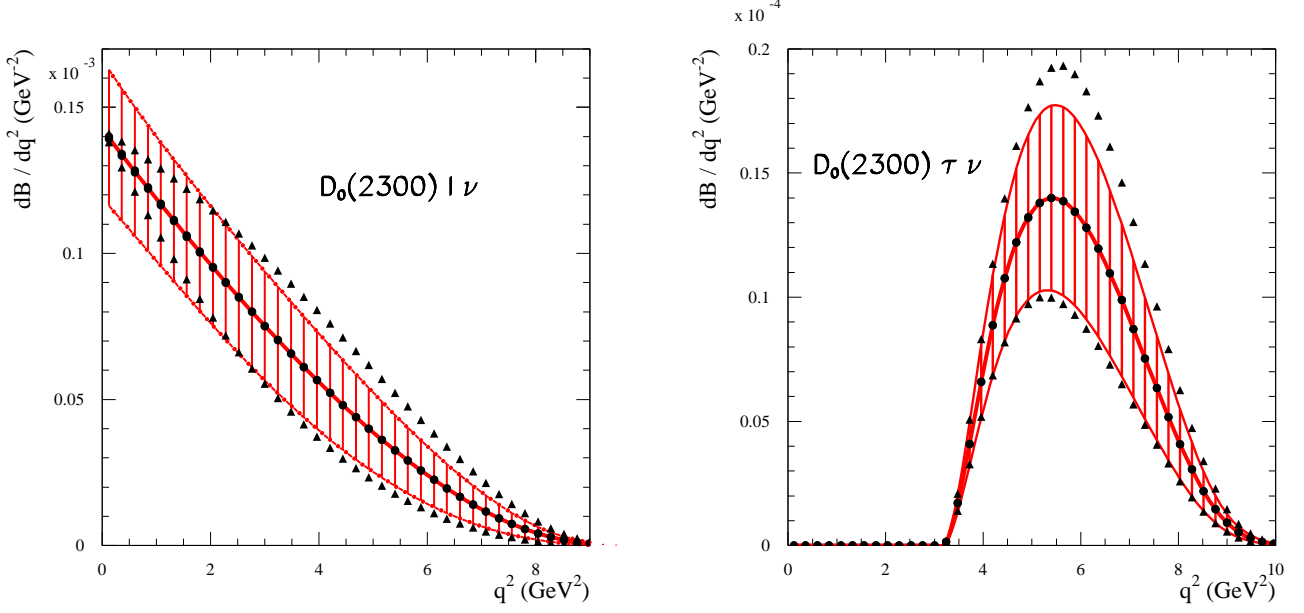


FIGURE 3. Expected q^2 distributions for $\overline{B}^0 \rightarrow D_0(2300)^+$ in semi-leptonic decays. Hatched areas correspond to uncertainties from the fit, curves with dots indicate the model uncertainty expected from $\hat{\tau}_2$ and $\hat{\eta}_2$ parameters whereas, those with triangles, correspond to the uncertainty from $\hat{\chi}_2$ and $\hat{\zeta}_1$. Other systematic uncertainties, invoked in Table XIII, are not displayed.

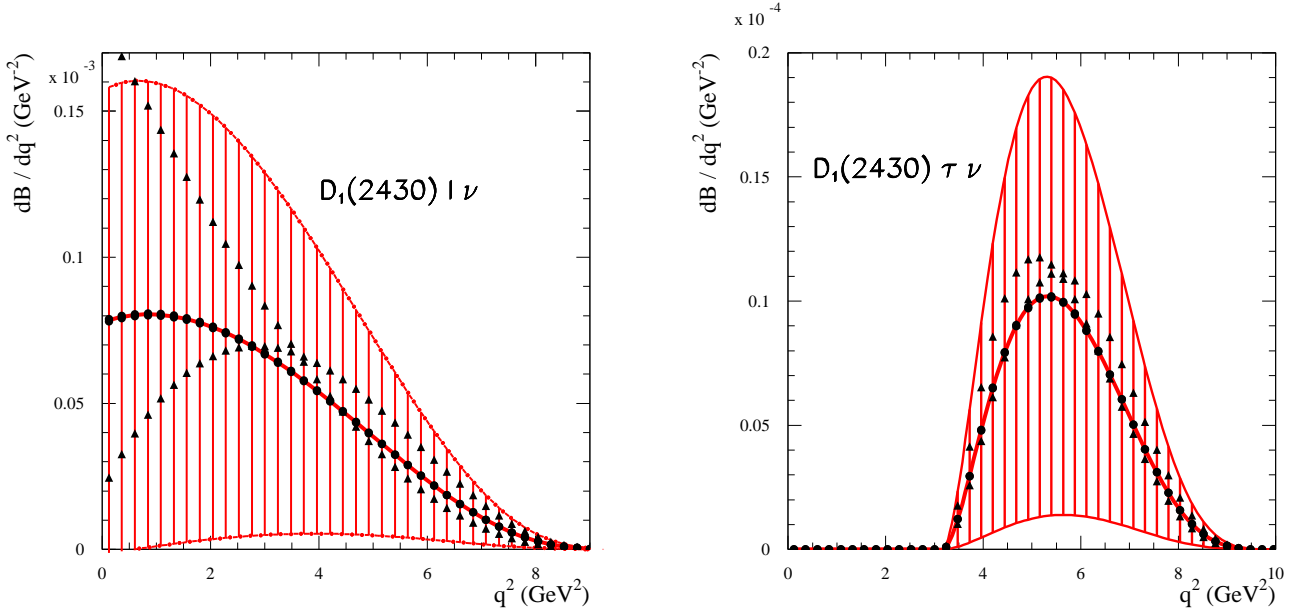


FIGURE 4. Expected q^2 distributions for $\overline{B}^0 \rightarrow D_1(2430)^+$ in semi-leptonic decays. Same conventions are used as in Fig.3

nic final states. We examine, in the following sections, if the contributions expected from $D_V^{(*)}$ components can fill these gaps. Such components have been ignored in pre-

vious analyses which consider that $D_{1/2}$ decays, alone, are enough to explain measurements.

B. Analysis and predictions for the $\overline{B}^0 \rightarrow D^* \pi \ell^- \bar{\nu}_\ell$ final state

We examine if measured $\overline{B}^0 \rightarrow D^* \pi \ell^- \bar{\nu}_\ell$ decays can be explained using a sum of D^{**} and $D_V^{(*)}$ components. All quoted numbers are relative to the sum of $D^{*0} \pi^+$ and $D^{*+} \pi^0$ final states and we refer to Section III B 2 for input measurements.

The measured branching fraction into broad components amounts to :

$$\mathcal{B}(\overline{B}^0 \rightarrow D^* \pi|_{\text{broad}} \ell^- \bar{\nu}_\ell) = (2.86 \pm 0.69) \times 10^{-3}. \quad (26)$$

In the hypothesis that contributions from higher mass resonances can be neglected, the expected contribution from $D_1(2430)^+$ decays, equal to $(0.46 \pm 0.46) \times 10^{-3}$, has to be complemented by a $D_V^{(*)}$ component equal to : $(2.4 \pm 0.8) \times 10^{-3}$. For r_{BW} values varying between 1 and 3 GeV^{-1} our estimates for this component are in the range $[2.0, 0.9] \times 10^{-3}$ (see Section III B 2). These values are compatible with the needed contribution.

In Figure 5, expected $D^* \pi$ mass distributions from our model (full line) and from the *LLSWBi* analysis (dashed line), are compared. To ease the comparison, central values expected from the two models are scaled to agree with the measured one. To do so, in our model, the $D_V^{(*)}$ component only is scaled while, for other components, expected values are used. In *LLSWBi*, the $D_1(2430)^+$ component, only, is scaled. Scaling factors are obtained for decays into light leptons and their values are used for the other analyzed transitions which involve a τ lepton or a D_s meson.

Spectra are dominated by the contributions from $D_{3/2}$ mesons.

1. Expected differences between our model and *LLSWBi*, for broad mass components

In the following we compare expected mass and q^2 distributions, for the $D^* \pi$ broad mass component, in our model and in *LLSWBi*, and after having normalized expectations to agree with the measured central value, for light leptons. Hatched areas correspond, only, to the uncertainty quoted in Eq. (26). Therefore, they are mainly indicative and do not illustrate the uncertainty on the shape of the distributions which comes from the model dependence of the two analyses.

For τ events one expects 1.3 times more events in our analysis whereas estimates were equal, by convention, for light leptons. This comes from the different dependence of $D_V^{(*)}$ and $D_1(2430)$ components versus q^2 . The $D_V^{(*)}$ component corresponds to a $D^* \pi$ mass distribution which can mimic a broad resonance in the absence of an analysis of the angular distribution.

C. Analysis and predictions for the $\overline{B}^0 \rightarrow D \pi \ell^- \bar{\nu}_\ell$ final state

All quoted numbers are relative to the sum of $D^0 \pi^+$ and $D^+ \pi^0$ final states. Input measurements are given in Section III B 1.

The measured branching fraction into broad components amounts to :

$$\mathcal{B}(\overline{B}^0 \rightarrow D \pi|_{\text{broad}} \ell^- \bar{\nu}_\ell) = (4.24 \pm 0.56) \times 10^{-3}. \quad (27)$$

In the hypothesis that contributions from higher mass resonances can be neglected, the expected contribution from $D_{1/2}$ decays is equal to $(0.51 \pm 0.24) \times 10^{-3}$. To account for the observed broad mass $D \pi$ distribution, the $D_0(2300)^+$ contribution has to be complemented by a D_V^* component equal to : $(3.7 \pm 0.6) \times 10^{-3}$. For r_{BW} values varying between 1 and 3 GeV^{-1} our estimates are in the range $[2.6, 1.5] \times 10^{-3}$. Therefore, taking into account present uncertainties, this scenario is compatible (marginally) with present measurements.

In Figure 8, we compare expected $D \pi$ mass distributions from our model (full line) and from the *LLSWBi* analysis (dashed line). There is a narrow peak from the D_2^{*+} meson located on top of a broad mass distribution which is very different in the two scenarios. As in the $D^* \pi$ channel analysis, broad mass distributions have been scaled so that total decay rates agree with measurements in the case of light leptons.

1. Expected differences between our model and *LLSWBi*, for broad mass components

In the following we compare expected mass and q^2 distributions, for the $D \pi$ broad mass component, in our model and *LLSWBi*, and after having normalized expectations to agree with the measured central value, for light leptons.

Our model and *LLSWBi* show marked differences. In particular, for τ events one expects two times more candidates in our model and very different mass and q^2 distributions. Dashed areas correspond to measured uncertainties of the broad mass component, used for the normalization, as given in Eq. (27) and do not include model uncertainties which can affect also the shape of the distributions.

X. PREDICTIONS FOR $\overline{B}^0 \rightarrow D^{**,+} D_s^-$ DECAYS

After having described our predictions for decay branching fractions of \overline{B}^0 mesons into the four $D^{**,+}$ accompanied by a D_s^- , we give expectations for the hadronic $D^* \pi$ and $D \pi$ final states.

Because the D_s meson and the τ lepton have a similar

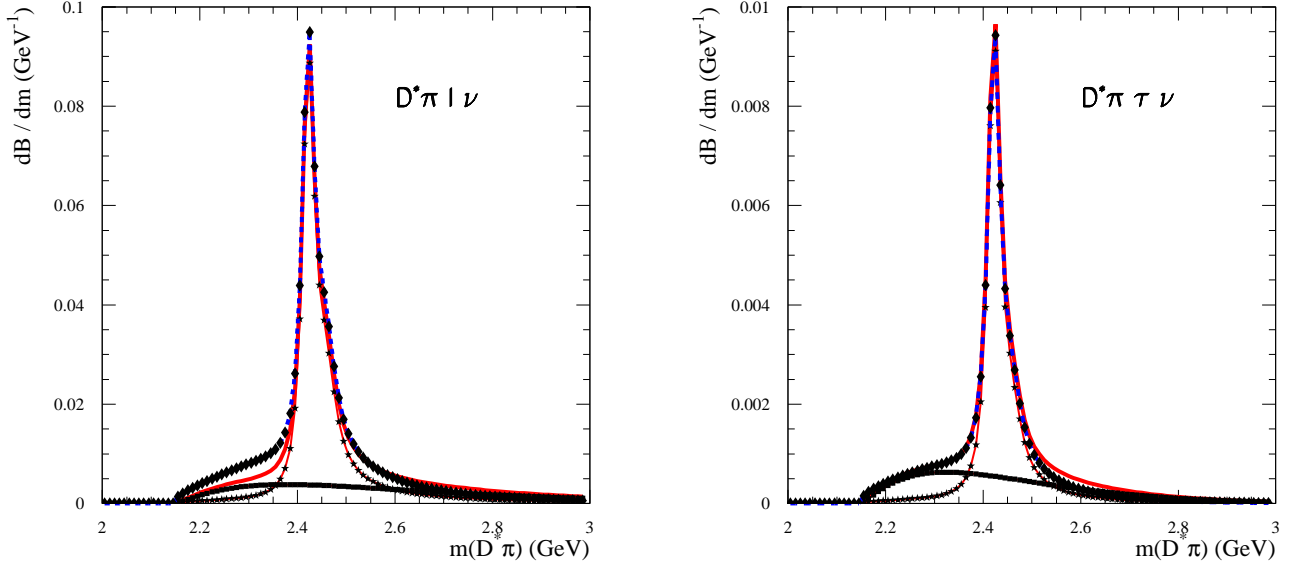


FIGURE 5. Expected $D^*\pi$ mass distributions for $\overline{B}^0 \rightarrow D^*\pi$ in semi-leptonic decays. Full lines correspond to our model and the dashed line is for $LLSWBi$. The line with stars gives the D^{**} contribution and the one with squares is for the $D_V^{(*)}$ component. The red line corresponds to the sum of these contributions. Only central values of the distributions are displayed.

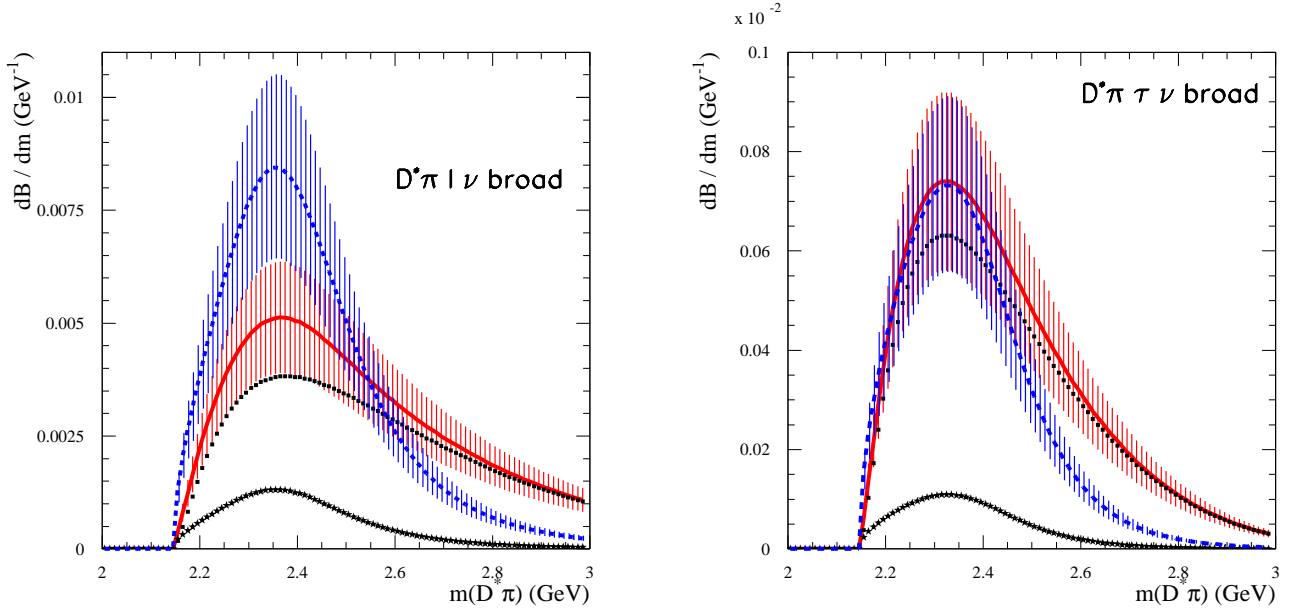


FIGURE 6. Expected broad $D^*\pi$ mass distributions for $\overline{B}^0 \rightarrow D^*\pi$ in semi-leptonic decays. The same conventions as in Figure 5 are used. Hatched areas include only the experimental uncertainty given in Eq. (26).

mass, we have also evaluated [30] the ratios :

$$\mathcal{R}_{D_i^{**}}^{\tau, D_s} = \frac{\mathcal{B}(\overline{B}^0 \rightarrow D_i^{**,+} \tau^- \bar{\nu}_\tau)}{\mathcal{B}(\overline{B}^0 \rightarrow D_i^{**,+} D_s^-)} \quad (28)$$

expecting that, because of correlations between the different sources of uncertainties, they are more accurate

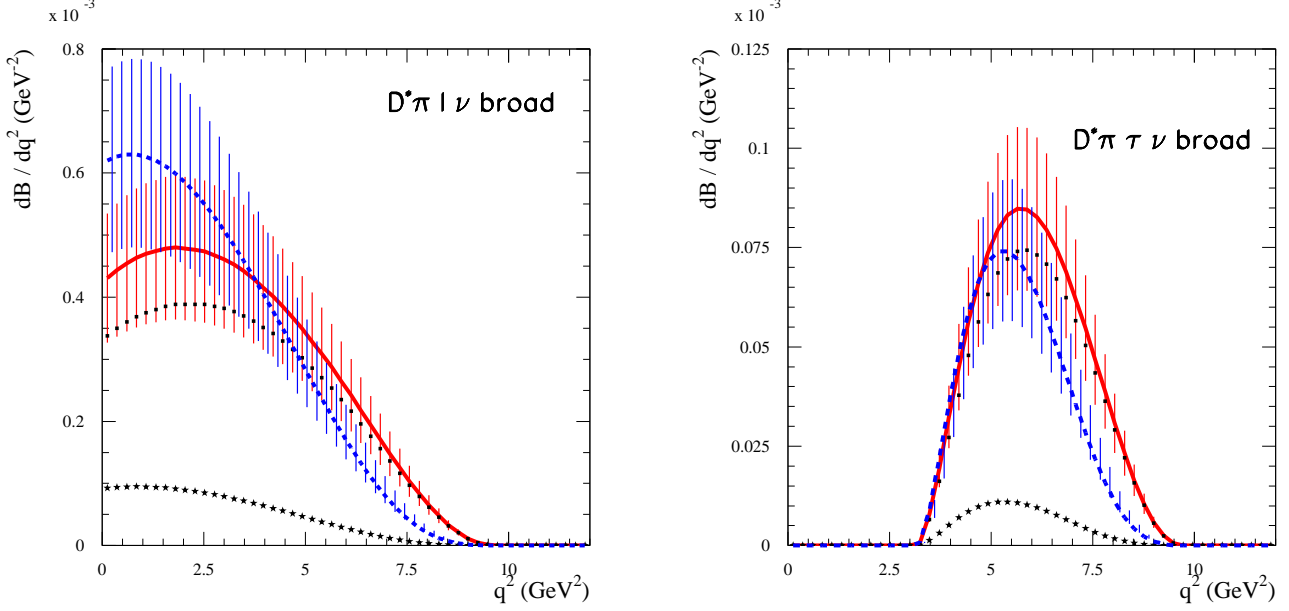


FIGURE 7. Expected q^2 distributions for $\overline{B}^0 \rightarrow D^*\pi$, broad mass component, in semi-leptonic decays. The same conventions as in Figure 5 are used.

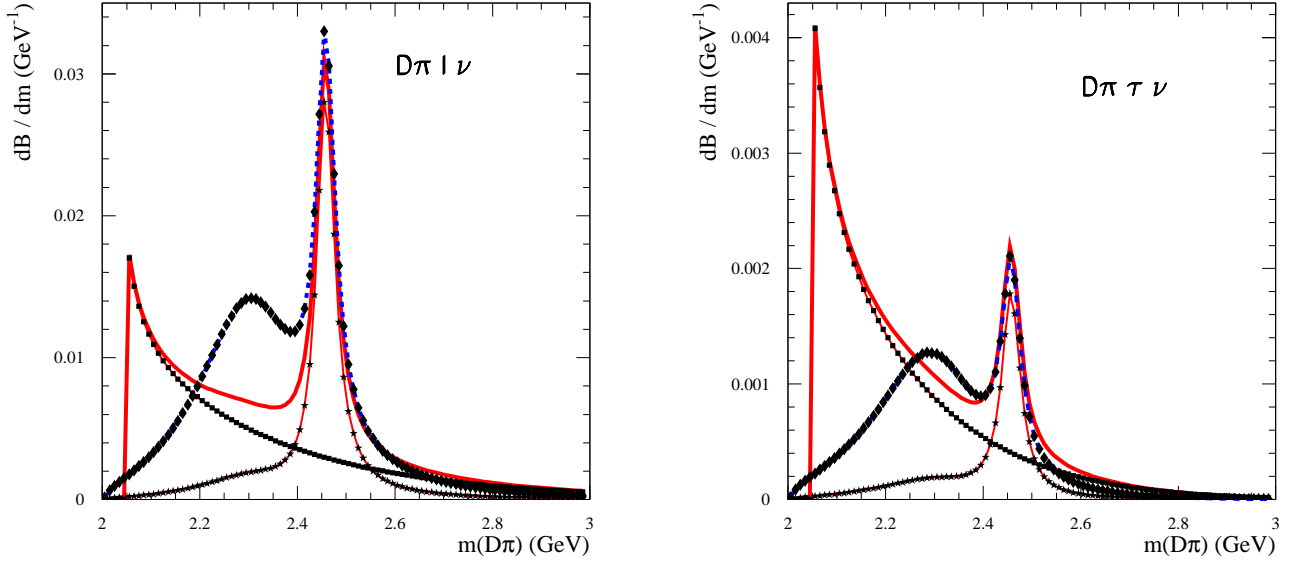


FIGURE 8. Expected $D\pi$ mass distributions for $\overline{B}^0 \rightarrow D\pi$ in semi-leptonic decays. Only central values are displayed.

than individual measurements of the corresponding decay rates, as observed already for semi-leptonic channels (see Table XIII).

Results can be used also for corresponding charged B -

meson decays, $B^- \rightarrow D^{**0} D_s^-$, because they are of Class I (once penguin terms are neglected). Branching fractions have simply to be corrected by the ratio between charged and neutral B -meson lifetimes and ratios $\mathcal{R}_{D_i^{**}}^{\tau, D_s}$ are the

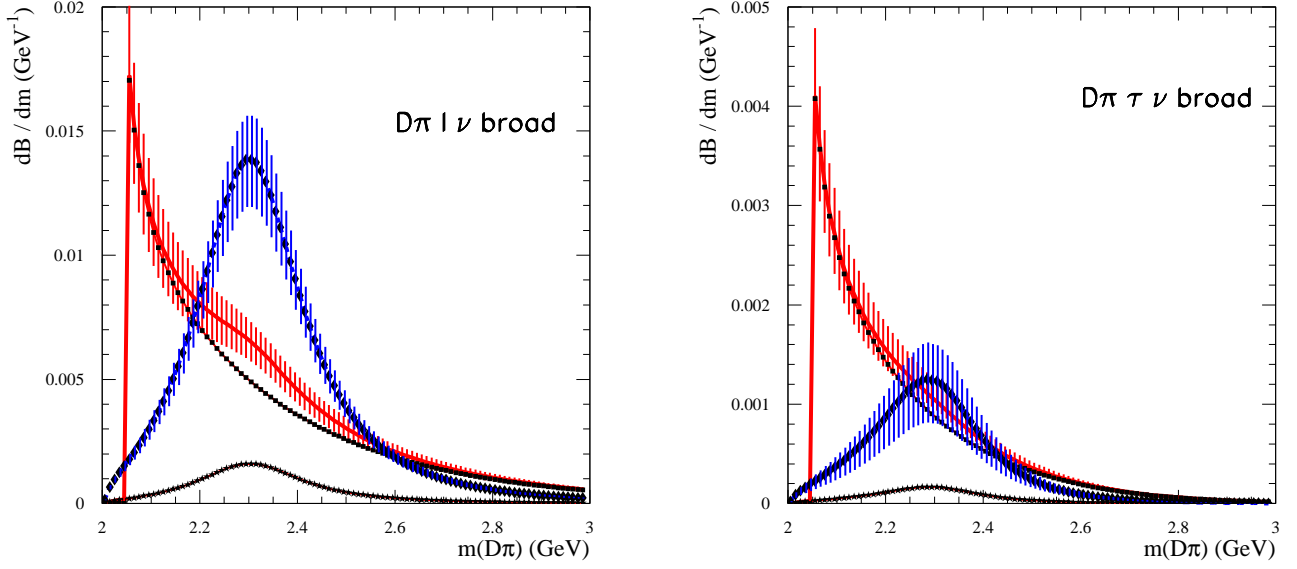


FIGURE 9. Expected broad $D\pi$ mass distributions for $\bar{B}^0 \rightarrow D\pi$ in semi-leptonic decays.

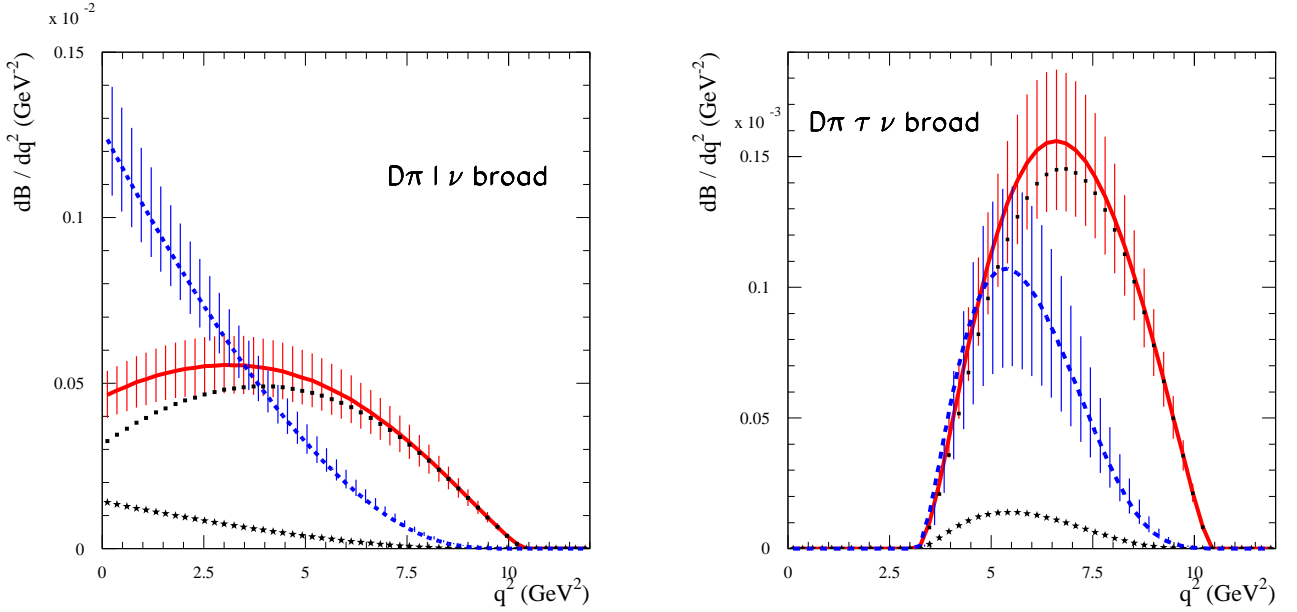


FIGURE 10. Expected q^2 distributions for $\bar{B}^0 \rightarrow D\pi$, broad mass component, in semi-leptonic decays.

same.

The validity of factorization in B meson decays, with emission of a heavy meson has been questioned, see the comment in Sec. II B supra, and the previous experimental tests had large uncertainties. Using $\mathcal{B}(\bar{B} \rightarrow D^{(*)}D_s^-)$

and $\mathcal{B}(\bar{B} \rightarrow D^{(*)}\ell^-\bar{\nu}_\ell)$ measurements, we have checked that this property is verified, once the evaluated contribution from penguin terms is taken into account. Therefore we use the same constraint, $a_{1,eff.} = 0.93 \pm 0.07$ and, in the absence of theoretical evaluations for penguin

amplitudes in $\bar{B} \rightarrow D^{**}D_s^-$ decays, we assume that they can be neglected.

A. Predicted values for $\mathcal{B}(\bar{B}^0 \rightarrow D_i^{**,+}D_s^-)$

Predicted values for $\bar{B}^0 \rightarrow D_i^{**,+}D_s^-$ decay branching fractions, in our model, are given in Table XIV.

channel	value \pm fit	model	HQET	IW linear	Blatt-W.
$\mathcal{B}(\bar{B}^0 \rightarrow D_2^{*+}D_s^-) \times 10^4$	5.8 ± 0.8	0.6	0.1	1.7	0.1
$\mathcal{R}_{D_2^*}^{\tau, D_s}$	0.33 ± 0.06	0.03	0.	-0.07	0.02
$\mathcal{B}(\bar{B}^0 \rightarrow D_1^+D_s^-) \times 10^4$	13.1 ± 3.5	0.9	-0.1	6.4	0.9
$\mathcal{R}_{D_1}^{\tau, D_s}$	0.48 ± 0.12	0.03	0.03	-0.15	-0.03
$\mathcal{B}(\bar{B}^0 \rightarrow D_0(2300)^+D_s^-) \times 10^4$	2.3 ± 0.4	0.2	0.1	0.2	0.0
$\mathcal{R}_{D_0(2300)}^{\tau, D_s}$	0.22 ± 0.04	0.05	-0.01	0.08	-0.03
$\mathcal{B}(\bar{B}^0 \rightarrow D_1(2430)^+D_s^-) \times 10^4$	1.4 ± 1.1	0.9	0.1	-0.1	0.
$\mathcal{R}_{D_1(2430)}^{\tau, D_s}$	0.25 ± 0.05	$^{+0.45}_{-0.10}$	0.01	0.04	-0.03

TABLE XIV. Our expectations for $\mathcal{B}(\bar{B}^0 \rightarrow D_i^{**,+}D_s^-)$ branching fractions, and their ratio, to corresponding semi-leptonic decays with a τ lepton. The first quoted uncertainty corresponds to the error from the fit. The model uncertainty is evaluated by changing the values of parameters, that are fixed to zero, by ± 0.5 GeV. Then, as explained in the text, are indicated variations of fitted parameters which correspond to different hypotheses that enter in the parameterization of fitted expressions.

Values obtained in the *LLSWBi* analysis are given in Table XIX in Appendix D 2.

Values for $D_1(2430)^+$ are very uncertain because of the lack of control of two parameters that enter in $1/m_Q$ corrections ($\hat{\chi}_2$ and $\hat{\zeta}_1$ in the present analysis). These model uncertainties affect also the ratio $\mathcal{R}_{D_1(2430)}^{\tau, D_s}$. Measurements of non-leptonic Class I B decays with $D_1(2430)$ emission are therefore desirable to improve the present situation.

To evaluate branching fractions when the hadronic final state, accompanying the D_s^- meson, is $D^*\pi$ or $D\pi$, we have to multiply values given in Table XIV for the production of the different D_i^{**} meson by corresponding branching fractions listed in Table VI. In our model we have also evaluated the $\bar{B}^0 \rightarrow D_V^{(*),+}D_s^-, D_V^{(*),+} \rightarrow D^{(*)}\pi$ expected contributions.

In practice it is not possible to compute really the expected mass distributions because of strong phase-shifts between the different hadronic amplitudes, that are unknown. One can evaluate only absolute values of these amplitudes. Therefore mass distributions, displayed in the following, are obtained by adding incoherently contributing individual channels.

B. Analysis of the $\bar{B}^0 \rightarrow D^*\pi D_s^-$ final state

All quoted numbers are relative to the sum of $D^{*0}\pi^+$ and $D^{*+}\pi^0$ final states. Expected branching fractions

for D^{**} channels, multiplied by $\mathcal{B}(D^{**} \rightarrow D^*\pi)$, are the following :

$$\begin{aligned} \mathcal{B}(\bar{B}^0 \rightarrow D_2^{*+}D_s^-) &= (2.3 \pm 0.3 \pm 0.2) \times 10^{-4} \\ \mathcal{B}(\bar{B}^0 \rightarrow D_1^+D_s^-) &= (8.8 \pm 2.3 \pm 0.6) \times 10^{-4} \\ \mathcal{B}(\bar{B}^0 \rightarrow D_1(2430)^+D_s^-) &= (1.4 \pm 1.1 \pm 0.9) \times 10^{-4} \quad (29) \end{aligned}$$

To evaluate the $D^*\pi$ mass distribution, D^{**} channels are complemented by the $D_V^{(*),+}$ contribution of $(3.0 \pm 1.0) \times 10^{-4}$. This gives a total broad $D^*\pi$ component of $(4.4 \pm 3.0) \times 10^{-4}$ which can be compared with the estimate from *LLSWBi* : $(8.8 \pm 7.4) \times 10^{-4}$.

It can be noted that the $D_V^{(*)}$ contribution can mimic a broad resonance and an analysis of the alignment distribution is necessary to separate the two possibilities.

C. Analysis of the $\bar{B}^0 \rightarrow D\pi D_s^-$ final state

All quoted numbers are relative to the sum of $D^0\pi^+$ and $D^+\pi^0/\gamma$ final states. Expected branching fractions for channels with a D^{**} meson, multiplied by $\mathcal{B}(D^{**} \rightarrow D\pi)$, are the following :

$$\begin{aligned} \mathcal{B}(\bar{B}^0 \rightarrow D_2^{*+}D_s^-) &= (3.48 \pm 0.46 \pm 0.33) \times 10^{-4} \\ \mathcal{B}(\bar{B}^0 \rightarrow D_0(2300)^+D_s^-) &= (2.30 \pm 0.43 \pm 0.22) \times 10^{-4} (30) \end{aligned}$$

To evaluate the $D\pi$ mass distribution, the D^{**} component is complemented by a D_V^* contribution evaluated

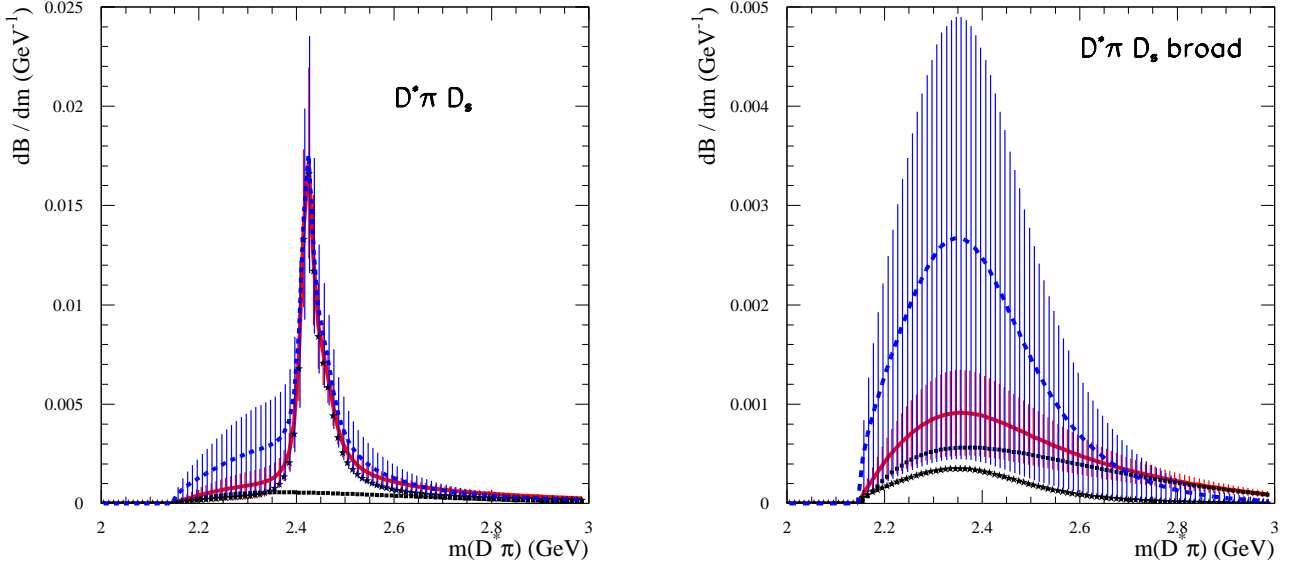


FIGURE 11. Expected $D^*\pi$ mass distributions from our analysis (full red curve) and from *LLSWBi* (dashed blue curve). Left plots correspond to all expected contributing components whereas the plots on the right are for broad mass components only.

to be $(5.5 \pm 0.9) \times 10^{-4}$. This gives a total broad $D\pi$ component of $(7.8 \pm 1.5) \times 10^{-4}$ which can be compared with the estimate from the *LLSWBi* analysis: $(17 \pm 8) \times 10^{-4}$.

XI. PREDICTIONS FOR $\bar{B}^0 \rightarrow D^{**,+} D_s^{*-}$ DECAYS

Expected results on decay branching fractions of \bar{B}^0 mesons into the four $D_i^{**,+}$ accompanied by a D_s^{*-} are given in Table XV, including different ratios that compare these branching fractions with those expected for $\bar{B}^0 \rightarrow D_i^{**,+} D_s^-$ and $\bar{B}^0 \rightarrow D_i^{**,+} \tau^- \bar{\nu}_\tau$ decays. Expressions for $\mathcal{B}(\bar{B}^0 \rightarrow D_i^{**,+} D_s^{*-})$ are given in Appendix A. They are obtained using factorization and considering only Class I decay amplitudes. These expressions are valid for charged or neutral B -meson decays.

$$\mathcal{R}_{D_i^{**} D_s^*}^{\tau, D_s^*} = \frac{\mathcal{B}(\bar{B}^0 \rightarrow D_i^{**,+} \tau^- \bar{\nu}_\tau)}{\mathcal{B}(\bar{B}^0 \rightarrow D_i^{**,+} D_s^{*-})} \quad (31)$$

and

$$\mathcal{R}_{D_i^{**} D_s^*}^{D_s, D_s^*} = \frac{\mathcal{B}(\bar{B}^0 \rightarrow D_i^{**,+} D_s^-)}{\mathcal{B}(\bar{B}^0 \rightarrow D_i^{**,+} D_s^{*-})} \quad (32)$$

channel	value \pm fit	model
$\mathcal{B}(\bar{B}^0 \rightarrow D_2^{*+} D_s^{*-}) \times 10^3$	1.9 ± 0.4	0.
$\mathcal{R}_{D_2^{*+} D_s^{*-}}^{\tau, D_s^*}$	0.100 ± 0.014	0.
$\mathcal{R}_{D_2^{*+} D_s^{*-}}^{D_s, D_s^*}$	0.30 ± 0.08	0.03
$\mathcal{B}(\bar{B}^0 \rightarrow D_1^{*+} D_s^{*-}) \times 10^3$	4.7 ± 0.9	0.1
$\mathcal{R}_{D_1^{*+} D_s^{*-}}^{\tau, D_s^*}$	0.134 ± 0.024	0.
$\mathcal{R}_{D_1^{*+} D_s^{*-}}^{D_s, D_s^*}$	0.28 ± 0.10	0.02
$\mathcal{B}(\bar{B}^0 \rightarrow D_0(2300)^+ D_s^{*-}) \times 10^4$	2.4 ± 0.7	1.0
$\mathcal{R}_{D_0(2300)^+ D_s^{*-}}^{\tau, D_s^*}$	0.20 ± 0.04	0.02
$\mathcal{R}_{D_0(2300)^+ D_s^{*-}}^{D_s, D_s^*}$	0.96 ± 0.26	$^{+0.44}_{-0.24}$
$\mathcal{B}(\bar{B}^0 \rightarrow D_1(2430)^+ D_s^{*-}) \times 10^4$	2.2 ± 2.0	$^{+0.6}_{-0.1}$
$\mathcal{R}_{D_1(2430)^+ D_s^{*-}}^{\tau, D_s^*}$	0.14 ± 0.02	0.02
$\mathcal{R}_{D_1(2430)^+ D_s^{*-}}^{D_s, D_s^*}$	0.52 ± 0.02	$^{+0.52}_{-0.36}$

TABLE XV. Our expectations for $\mathcal{B}(\bar{B}^0 \rightarrow D_i^{**,+} D_s^{*-})$ branching fractions, and their ratio, to corresponding semi-leptonic decays with a τ lepton and non-leptonic D_s^- production. The first quoted uncertainty corresponds to the error from the fit. The model uncertainty is evaluated by changing the values of parameters, that are fixed to zero, by ± 0.5 GeV.

XII. CONCLUSIONS

We have analyzed $\bar{B} \rightarrow D^{**}$ decays in semi-leptonic and non-leptonic Class I processes that can be related

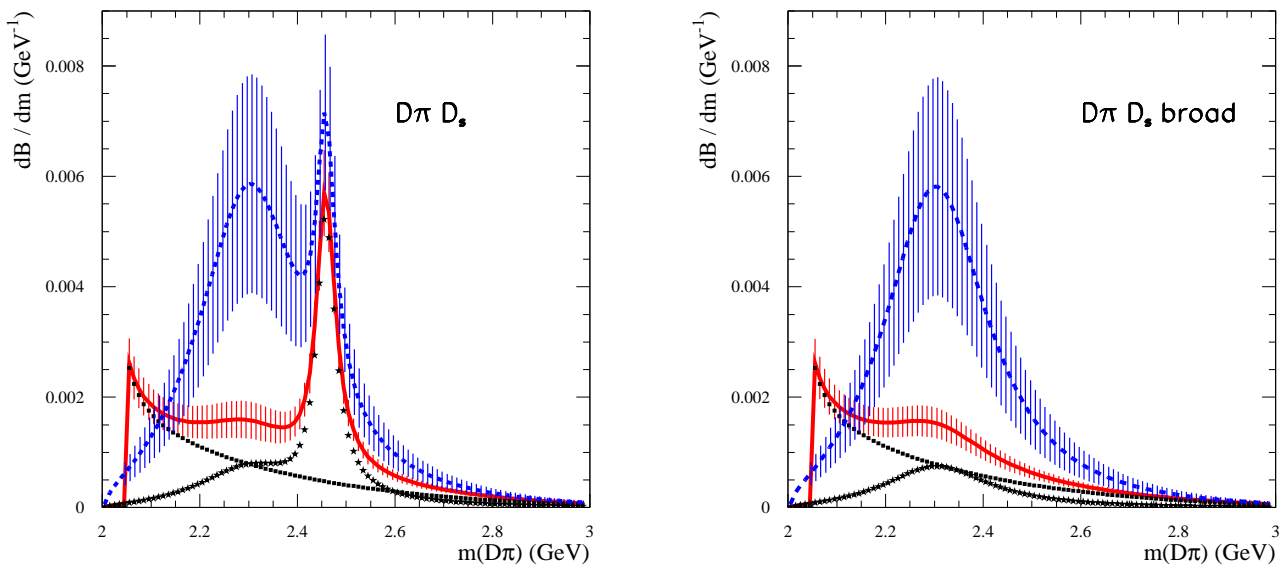


FIGURE 12. Expected $D\pi$ mass distributions obtained in our model (red full line) and in *LLSWBi* (blue dashed line). Left plots correspond to all expected contributing components whereas, plots in the right are for broad mass components only.

using factorization.

We have verified that factorization is well satisfied in $\bar{B} \rightarrow D_{3/2}$ decays and also in Class I non-leptonic transitions with D_s^- emission.

Assuming naturally that this factorization is valid also in $\bar{B} \rightarrow D_{1/2}$ decays, one expects a quite small contribution from $D_{1/2}$ relative to $D_{3/2}$ mesons in semi-leptonic decays as is the case in non-leptonic Class I processes. This is in contrast with the results of *LLSWBi* and in agreement with LQCD computations of the corresponding IW functions at maximum transfer [9] and with relativistic QM calculations [14].

To evaluate branching fractions for the different decay channels in which a D^{**} meson is produced, we use the expressions derived in [3]. They depend on several parameters that control $1/m_Q$ corrections. Using present experimental measurements and constraints from theory we have determined the most important of these parameters for $D_{3/2}$ emission. In particular we find that the $1/m_Q$ correction $\hat{e}_{3/2}$ included in the auxiliary $\tau_{3/2}^{eff}$, is of the order of -0.2 ± 0.1 , the minus sign confirming the agreement with a quark model calculation. The three other quantities we obtain are of the order of $\bar{\Lambda}$, as expected in a $1/m_Q$ expansion, which is encouraging in view of the roughness of the method. For $D_{1/2}$ mesons, estimates of the parameters are more uncertain but this does not change our conclusion on the smallness of the contribution.

To explain measurements of exclusive $D^{(*)}\pi$ broad hadronic final states in B meson semi-leptonic decays we

have evaluated the contribution from $D_V^{(*)}$ components, in addition to $D_{1/2}$ decays. These components can be normalized by using $\bar{B} \rightarrow D^{(*)}\ell^- \bar{\nu}_\ell$ measurements but the mass dependence of the $D^{(*)}\pi$ mass distribution remains highly undetermined.

We propose a model which accounts for $\bar{B} \rightarrow D^{(*)}\pi\ell^- \bar{\nu}_\ell$ measurements by adding $D_V^{(*)}$ and D^{**} contributions. We have, at present, not considered contributions from higher mass hadronic states. Results have been compared with the *LLSWBi* model in which $D_{1/2}$ mesons alone explain the broad mass spectra.

These two models give very different expectations for the broad $D^{(*)}\pi$ mass and q^2 distributions regarding light leptons. The $D\pi$ final state, in particular can provide clear informations on the relative importance of the D_V^* and $D_0(2300)$ components. The two models have also very different expectations for semi-leptonic decays with a τ lepton and in Class I non-leptonic transitions with $D_s^{(*)}$ emission.

Annexe A: Expressions for Class I non-leptonic decays

Expressions for Lorentz invariant form factors are those of *LLSW* [3], therefore, for the IW functions, one has to use the correspondance $\tau(w) = \sqrt{3}\tau_{3/2}(w)$ and $\zeta(w) = 2\tau_{1/2}(w)$. In following formulas, Lorentz invariant form-factors are evaluated at $w_D = (m_B^2 - m_{P(V)}^2) +$

$m_{D^{**}}^2)/(2m_B m_{D^{**}})$ while the quantity w , which appears in the rest of the expressions, is computed at the running mass value of the D^{**} resonance. Expressions for the traditional Blatt-Weisskopf damping factors in $\bar{B} \rightarrow D^{**} X$ decays in which X is a stable particle and which occur in an angular momentum $L = 1, 2,$ and 3 are the following :

$$\begin{aligned} F_{B,1}(p') &= \frac{1}{\sqrt{1+z}} \\ F_{B,2}(p') &= \frac{1}{\sqrt{9+3z+z^2}} \\ F_{B,3}(p') &= \frac{1}{\sqrt{225+45z+6z^2+z^3}} \end{aligned} \quad (\text{A1})$$

with $z = (r_{BW} p')^2$, in which p' is the decay momentum evaluated in the \bar{B} rest-frame. For the damping term, we use $r_{BW} = 3 (GeV)^{-1}$. We define the quantities :

$$B_{B,L}(w) = \left(\frac{F_{B,L}(p')}{F_{B,L}(p'_0)} \right)^2 \quad (\text{A2})$$

that are the ratios of the previous functions evaluated at the running mass of the D^{**} resonance and at its nominal mass, $m_{D^{**}}$.

1. $\bar{B}^0 \rightarrow D^{**,+} P^-$ decays

We write the following expressions for a generic pseudo-scalar meson denoted as " P ". $a_{1,eff}^{D^{**},P}$ is an effective parameter describing the deviation from strict factorization which includes also possible contributions from exchange, annihilation or penguin amplitudes, $V_{q_1 q_2}$ is the relevant light-quarks CKM matrix element and f_P the annihilation constant. Those parameters are to be adapted to the case under consideration.

The damping factor $B_{B,2}(w)$ is used for $\bar{B} \rightarrow D_{3/2}$ decays, that occur in a D-wave and, as usual, no damping is considered for the decays into $D_{1/2}$ states, that are S-wave. Each expression is followed by its $m_Q = \infty$ limit (between parentheses). This is valid also in the case of a final vector meson.

$$\begin{aligned} \Gamma_{\bar{B}^0 \rightarrow D_2^{*+} P^-} &= |a_{1,eff}^{D_2^*,P}|^2 |V_{cb} V_{q_1 q_2}^*|^2 \frac{G_F^2}{24\pi} f_P^2 m_B m_{D_2^*}^2 |k_{A_1} + k_{A_2}(1-rw) + k_{A_3}(w-r)|^2 (w^2-1)^{5/2} B_{B,2}(w) \\ &(|a_{1,eff}^{D_2^*,P}|^2 |V_{cb} V_{q_1 q_2}^*|^2 \frac{G_F^2}{24\pi} f_P^2 m_B m_{D_2^*}^2 \tau(w)^2 (1-r)^2 (1+w)^2 (w^2-1)^{3/2} \text{ in the } m_Q \rightarrow \infty \text{ limit}) \end{aligned}$$

$$\begin{aligned} \Gamma_{\bar{B}^0 \rightarrow D_1^+ P^-} &= |a_{1,eff}^{D_1^*,P}|^2 |V_{cb} V_{q_1 q_2}^*|^2 \frac{G_F^2}{16\pi} f_P^2 m_B m_{D_1^*}^2 |f_{V_1} + f_{V_2}(1-rw) + f_{V_3}(w-r)|^2 (w^2-1)^{3/2} B_{B,2}(w) \\ &(|a_{1,eff}^{D_1^*,P}|^2 |V_{cb} V_{q_1 q_2}^*|^2 \frac{G_F^2}{24\pi} f_P^2 m_B m_{D_1^*}^2 \tau^2 (1-r)^2 (1+w)^2 (w^2-1)^{3/2}) \end{aligned}$$

$$\begin{aligned} \Gamma_{\bar{B}^0 \rightarrow D_0(2300)^+ P^-} &= |a_{1,eff}^{D_0^*,P}|^2 |V_{cb} V_{q_1 q_2}^*|^2 \frac{G_F^2}{16\pi} f_P^2 m_B m_{D_0^*}^2 |g_+(1-r)(1+w) + g_-(1+r)(1-w)|^2 (w^2-1)^{1/2} \\ &(|a_{1,eff}^{D_0^*,P}|^2 |V_{cb} V_{q_1 q_2}^*|^2 \frac{G_F^2}{16\pi} f_P^2 m_B m_{D_0^*}^2 \zeta^2 (1+r)^2 (1-w)^2 (w^2-1)^{1/2}) \end{aligned}$$

$$\begin{aligned} \Gamma_{\bar{B}^0 \rightarrow D_1^{*+} P^-} &= |a_{1,eff}^{D_1^*,P}|^2 |V_{cb} V_{q_1 q_2}^*|^2 \frac{G_F^2}{16\pi} f_P^2 m_B m_{D_1^*}^2 (w^2-1)^{3/2} |g_{V_1} + g_{V_2}(1-rw) + g_{V_3}(w-r)|^2 \\ &(|a_{1,eff}^{D_1^*,P}|^2 |V_{cb} V_{q_1 q_2}^*|^2 \frac{G_F^2}{16\pi} f_P^2 m_B m_{D_1^*}^2 (1-r)^2 \zeta^2 (w^2-1)^{3/2}) \end{aligned}$$

2. $\bar{B}^0 \rightarrow D^{**,+} V^-$ decays

These expressions are obtained by a direct calculation.

Several partial waves are contributing in each decay channel and the appropriate Blatt and Weisskopf damping factor has to be used for each contribution. It can be identified from the power of the momentum dependence.

$$\begin{aligned} \Gamma_{\bar{B}^0 \rightarrow D_2^{*+} V^-} &= |a_{1,eff}^{D_2^*,V}|^2 |V_{cb} V_{q_1 q_2}^*|^2 \frac{G_F^2}{48\pi} f_V^2 \frac{m_V^2 m_{D_2^*}^2}{m_B} (w^2-1)^{3/2} [3|k_V|^2 (w^2-1) B_{B,2}(w) \\ &+ |k_{A_1}|^2 \left(5 B_{B,1}(w) + 2 \frac{m_P^2}{m_V^2} (w^2-1) B_{B,2}(w) \right) + 2|k_{A_2} + \frac{1}{r} k_{A_3}|^2 (w^2-1)^2 \frac{m_{D_2^*}^2}{m_V^2} B_{B,3}(w) \\ &+ 4 \text{Re}(k_{A_1}^* (k_{A_2} + \frac{1}{r} k_{A_3})) (w^2-1) (w-r) \frac{m_B m_{D_2^*}}{m_V^2} \sqrt{B_{B,1}(w)} \sqrt{B_{B,3}(w)}] \\ &(|a_{1,eff}^{D_2^*,V}|^2 |V_{cb} V_{q_1 q_2}^*|^2 \frac{G_F^2}{48\pi} f_V^2 \frac{m_V^2 m_{D_2^*}^2}{m_B} \tau^2 (5(1+w)^2 + (w^2-1)(3 + 4 \frac{m_B m_D}{m_V^2} (1+w))) (w^2-1)^{3/2}) \end{aligned}$$

$$\Gamma_{\bar{B}^0 \rightarrow D_1^+ V^-} = |a_{1,eff}^{D_1^*,V}|^2 |V_{cb} V_{q_1 q_2}^*|^2 \frac{G_F^2}{16\pi} f_V^2 m_V^2 m_{D_1^*}^2 / m_B (w^2-1)^{1/2} \left[|f_{V_1}|^2 (3 + \frac{m_P^2}{m_V^2} (w^2-1) B_{B,1}(w)) \right]$$

$$\begin{aligned}
& +2|f_A|^2(w^2 - 1)B_{B,1}(w) + |f_{V_2} + \frac{1}{r}f_{V_3}|^2(w^2 - 1)^2\frac{m_{D_1}^2}{m_V^2}B_{B,2}(w) \\
& +2Re(f_{V_1}^*(f_{V_2} + \frac{1}{r}f_{V_3}))(w^2 - 1)(w - r)\frac{m_B m_{D_1}}{m_V^2}\sqrt{B_{B,1}(w)}\sqrt{B_{B,2}(w)} \\
& (|a_{1,eff}^{D_1,V}|^2|V_{cb}V_{q_1q_2}^*|^2\frac{G_F^2}{96\pi}f_V^2\frac{m_V^2 m_{D_1}^2}{m_B}\tau^2\left[2(1+w)^2 + (w^2 - 1)(3 + \frac{m_B^2}{m_V^2}(2r(1+w) + 3(1+r)^2))\right] \\
& (w^2 - 1)^{3/2})
\end{aligned}$$

$$\begin{aligned}
\Gamma_{\overline{B}^0 \rightarrow D_0(2300)+V^-} & = |a_{1,eff}^{D_0^*,V}|^2|V_{cb}V_{q_1q_2}^*|^2\frac{G_F^2}{16\pi}f_V^2\frac{m_{D_0^*}^4}{m_B}(w^2 - 1)^{3/2}|g_+(1 + \frac{1}{r}) + g_-(1 - \frac{1}{r})|^2B_{B,1}(w) \\
& (|a_{1,eff}^{D_0^*,V}|^2|V_{cb}V_{q_1q_2}^*|^2\frac{G_F^2}{16\pi}f_V^2m_{D_0^*}^4/m_B\zeta^2(1 - 1/r)^2(w^2 - 1)^{3/2})
\end{aligned}$$

$$\begin{aligned}
\Gamma_{\overline{B}^0 \rightarrow D_1^+V^-} & = |a_{1,eff}^{D_1^*,V}|^2|V_{cb}V_{q_1q_2}^*|^2\frac{G_F^2}{16\pi}f_V^2\frac{m_V^2 m_{D_1^*}^2}{m_B}(w^2 - 1)^{1/2}\left[|g_{V_1}|^2(3 + \frac{m_B^2}{m_V^2}(w^2 - 1)B_{B,1}(w)) + \right. \\
& 2|g_A|^2(w^2 - 1)B_{B,1}(w) + |g_{V_2} + \frac{1}{r}g_{V_3}|^2(w^2 - 1)^2\frac{m_{D_1^*}^2}{m_V^2}B_{B,2}(w) \\
& \left. +2Re(g_{V_1}^*(g_{V_2} + \frac{1}{r}g_{V_3}))(w^2 - 1)(w - r)\frac{m_B m_{D_1^*}}{m_V^2}\sqrt{B_{B,1}(w)}\sqrt{B_{B,2}(w)}\right] \\
& (|a_{1,eff}^{D_1^*,V}|^2|V_{cb}V_{q_1q_2}^*|^2\frac{G_F^2}{16\pi}f_V^2m_B m_{D_1^*}^2\zeta^2(3(m_V/m_B)^2(w - 1)/(w + 1) + 2((1 - r)^2 + r(1 - w)))(w^2 - 1)^{3/2})
\end{aligned}$$

Annexe B: Calculations of $\eta_{ke}^{b(c)}$ and η^b with NR treatment of the c.o.m motion

1) according to the standard analysis, the $\mathcal{O}(1/m_Q)$ corrections to form factors fall into two main categories, due to modifications of :

- the state vectors ;
- the current operators.

Here we are concerned with the first category, and the η 's or χ 's parameters are precisely characterizing the corrections to the form factors due to this modification of state vectors, when the current operator is kept to the infinite mass limit.

More precisely, we want to consider $\eta_{ke}^{b(c)}$, which parameterize the effect of the kinetic operator \mathcal{O}_{ke} on respectively the initial ground state and on the $j = 3/2$ final state, with specification to $w = 1$.

2) in terms of the quark model, the modification of vector states at $w = 1$ is identified with the one of the rest frame wave functions of the mesons, and the aim is then to evaluate the effect of this modification on form factors, i.e. on matrix elements of currents when the current **operator** is kept to its infinite mass limit.

As concerns $\eta_{ke}^{b(c)}$, one can give an intuitive interpretation by assuming that they are generated by the addition of the heavy quark kinetic energy in the Schrödinger equation :

$$p^2/2m_q \rightarrow p^2/2m_q + p^2/2m_Q$$

m_q, m_Q being respectively the light and heavy quark masses. But this amounts simply to replace m_q by the reduced mass $\mu = \frac{m_q m_Q}{m_q + m_Q}$:

$$p^2/2m_q \rightarrow p^2/2\mu$$

This fact implies that the wave equation is the same as in the heavy quark limit, except for the change of mass. In the case of power-like potential r^α , this allows to use the scale invariance to deduce the wave functions from the heavy mass limit ones ϕ^∞ . Let the equation be :

$$(p^2/2m_q + br^\alpha)\phi^\infty(\vec{r}) = E_n\phi^\infty(\vec{r})$$

Performing the substitution $\vec{r} \rightarrow \lambda\vec{r}$, one has :

$$(\frac{p^2}{2m_q\lambda^{2+\alpha}} + br^\alpha)\phi^\infty(\lambda\vec{r}) = \frac{E_n}{\lambda^\alpha}\phi^\infty(\lambda\vec{r})$$

Therefore if one chooses $\lambda = (\mu/m_q)^{1/(2+\alpha)} = (1 + (m_q/m_Q))^{(-1/(2+\alpha))}$, one sees that $\phi^\infty(\lambda\vec{r})$ is the solution of the finite mass equation. The normalised wave function is :

$$\lambda^{3/2}\phi^\infty(\lambda\vec{r}).$$

Now, the non relativistic (NR) (in fact the familiar dipolar expression) for τ is :

$$\tau(w = 1) = m(\phi_f^\infty|z|\phi_i^\infty)$$

Note that $j=1/2$ and $j=3/2$ are degenerate at $m_Q = \infty$ in the NR approach (no Wigner rotation) if one disregards any spin-orbit force. In fact, all the spin dependent forces are relativistic effects in the sense that they are $\mathcal{O}(v^2/c^2)$ with respect to internal velocities. Therefore, even at finite m_Q , if one considers the fully NR approach, there are no spin independent forces. This is what is done in the following paragraphs 1),2),3) below where we mean only to evaluate **kinetic energy** corrections to B and $D^{(**)}$.

On the other hand, for η^b , which combines all the type of η 's relative to the B , one has to consider the spin-dependent forces, since this contains the magnetic contributions generating the η 's (1,2,3). This is done in paragraph 4), where we use the GI model which contains all the relevant forces. An important contribution is obviously the one of spin-spin force, although it is $1/m_Q$. It lifts the degeneracy with the B^* .

We now define :

$$\tau^{b,c}(w=1) = m(\phi_f^c | z | \phi_i^b),$$

with the substitution by the finite mass wave functions, whence the corrections are represented by [?] :

$$\tau^{b,c}(w=1) - \tau(w=1) \quad (\text{B1})$$

or, assuming the proportionality to the τ and defining reduced corrections as $\hat{\eta}$,

$$\begin{aligned} \tau^{b,c}(w=1)/\tau(w=1) &= 1 + \frac{\hat{\eta}_{ke}^b}{2m_b} + \frac{\hat{\eta}_{ke}^c}{2m_c} + \dots \\ &= \lambda_b^{3/2} \lambda_c^{3/2} \frac{\int d_3\vec{r} z \phi_1^\infty(\lambda_c \vec{r}) \phi_0^\infty(\lambda_b \vec{r})}{\int d_3\vec{r} z \phi_1^\infty(\vec{r}) \phi_0^\infty(\vec{r})} \quad (\text{B2}) \end{aligned}$$

where 0, 1 denote the orbital angular momentum L . If one passes to radial wave functions by means of an angular integration :

$$\tau^{b,c}(w=1)/\tau(w=1) = \lambda_b^{3/2} \lambda_c^{3/2} \frac{\int r^3 dr \phi_1^\infty(\lambda_c r) \phi_0^\infty(\lambda_b r)}{\int r^3 dr \phi_1^\infty(r) \phi_0^\infty(r)}$$

If one makes $m_b = m_c = m_Q$, one finds :

$$\tau^{b,c}(w=1)/\tau(w=1) = 1 + \frac{\hat{\eta}_{ke}^b}{2m_Q} + \frac{\hat{\eta}_{ke}^c}{2m_Q} + \dots \quad (\text{B3})$$

$$= 1/\lambda_Q = 1 + \frac{m_q/m_Q}{2+\alpha} + \dots \quad (\text{B4})$$

$$\hat{\eta}_{ke}^b + \hat{\eta}_{ke}^c = \frac{2m_q}{2+\alpha}$$

To go further and separate $\hat{\eta}_{ke}^b$ and $\hat{\eta}_{ke}^c$, one needs explicit wave functions, which is possible for $\alpha = 2$ (harmonic oscillator) or -1 (Coulomb).

Harmonic oscillator ($\alpha = 2$) : $\phi_0^\infty(r) \propto e^{(-r^2/(2R^2))}$, $\phi_1^\infty(r) \propto r e^{-r^2/(2R^2)}$

$$\tau^{\infty,c}(w=1)/\tau(w=1) = \left(\frac{2\lambda_c}{\lambda_c^2 + 1} \right)^{5/2} \quad (\text{B5})$$

whence $\hat{\eta}_{ke}^c = 0$, and $\hat{\eta}_{ke}^b = (2m_q)/(2+2) = m_q/2$

Coulomb ($\alpha = -1$) : $\phi_0^\infty(r) \propto e^{(-r/r_0)}$, $\phi_1^\infty(r) \propto r e^{(-r/2r_0)}$

$$\tau^{\infty,c}(w=1)/\tau(w=1) = \left(\frac{3\lambda_c^{1/2}}{\lambda_c^2 + 2} \right)^5 \quad (\text{B6})$$

whence $\hat{\eta}_{ke}^c = -10/6 m_q$, and $\hat{\eta}_{ke}^b = (2m_q)/(2-1) + 10/6 m_q = 11/3 m_q$.

3) numerical calculation for a linear+Coulomb potential

Of course, the physical potential is rather of linear+Coulomb type. The result may be expected to lay between the HO and the Coulomb one. But one has no analytical solution. Therefore we perform a numerical calculation, using the particular wave functions of reference [32] with a potential close to linear+Coulomb and find, with m_Q respectively infinite or equal to $5 GeV$ masses (light mass : $m_q = 0.45 GeV$)[?] :

$$\tau^{m_b=5, m_c=\infty}(w=1)/\tau(w=1) = 1 + \frac{\hat{\eta}_{ke}^b}{2m_b} = 1.053 \quad (\text{B7})$$

$$\tau^{m_b=\infty, m_c=5}(w=1)/\tau(w=1) = 1 + \frac{\hat{\eta}_{ke}^c}{2m_c} = 0.9898 \quad (\text{B8})$$

$$\tau^{m_b=5, m_c=5}(w=1)/\tau(w=1) = 1 + \frac{\hat{\eta}_{ke}^b + \hat{\eta}_{ke}^c}{2m_Q} = 1.045 \quad (\text{B9})$$

whence approximately : $\hat{\eta}_{ke}^b \simeq 0.5 GeV$, $\hat{\eta}_{ke}^c \simeq -0.1 GeV$, which is indeed intermediate between the results from HO and Coulomb potentials. In fact $\hat{\eta}_{ke}^b + \hat{\eta}_{ke}^c \simeq 0.5 GeV$ corresponds roughly to what is expected from $\alpha = 0$ (Eq. above), i.e. m_q , and it is indeed well known that such a power potential $\alpha \simeq 0$ or a log one approximate roughly the linear+Coulomb one (e.g. Martin potentials).

The conclusion up to now is that $\hat{\eta}_{ke}^c < 0$. In addition, $\hat{\eta}_{ke}^b > 0$ but what must be estimated is $\hat{\eta}^b$, a common combination appearing in all the form factors, and which can therefore be interpreted as the effect of the full Lagrangian contribution, i.e., intuitively, one needs to include spin dependent forces, which are not present in the potentials which have been considered up to now.

4) numerical calculation of $\hat{\eta}^b$ for the GI model.

We consider then the Godfrey and Isgur spectroscopic model with all relevant forces, and moreover a relativistic kinetic energy. To obtain $\hat{\eta}^b$, we calculate the variation of τ with the initial B respectively at infinite and finite mass. We find finally $\hat{\eta}^b \simeq -0.26 GeV$: this indicates that the effect of spin-spin force is large, dominating the kinetic energy effect.

Annexe C: Repeating the *LLSWB* analysis of [4, 5]

This comparison is intended to show that, using the same input data and constraints we find, using our own code, the same values for fitted parameters as in [4, 5], with the *LLSWB* approach.

For this purpose measurements of B -meson semi-leptonic decays and $\bar{B}^0 \rightarrow D_{3/2}^+ \pi^-$ non-leptonic decays, reported in the third column of Table IV, are used to constrain parameterizations of hadronic form factors. In addition, measurements from Belle [8] which provide, respectively, 4 and 5 values for the production fractions of D_2^* and $D_0(2300)$ mesons, in different bins of the w variable are used. The w dependence of the two IW functions is assumed to be linear. The validity of factorization

, with $a_1 = 1$, is assumed, to relate semi and non-leptonic decays in which $D_{3/2}$ mesons, only, are emitted.

Therefore $\overline{B}^0 \rightarrow D_{1/2}^+ \pi^-$ non-leptonic decays are not included in the analysis. D^{**} mesons are assumed to be stable (no mass distribution is considered).

We have modified accordingly our analysis but some differences remain :

- for the fractions measured in different w bins, we have not used one of the measurements in each of the two samples because these quantities are not independent (their sum is equal to one);
- the parameterization of the different form factors is derived from the original article of [3], without using different approximations;
- in addition to α_s corrections, we have also included, for $D_{3/2}$ mesons, those at order $1/m_Q \times \alpha_s$, provided in [3];

1. Numerical aspects

Production of $D_{3/2}$ and $D_{1/2}$ mesons are evaluated separately. In addition to the normalization and slope of the IW functions, the same parameters which determine $1/m_Q$ corrections, as in [5], are fitted.

Considering $D_{3/2}$ mesons only, values of fitted parameters are compared in Table XVI.

We obtain very similar results. The numbers of degree of freedom differ by one unit, in the two analyses, because we have not used one of the measurements for the w dependence of D_2^* production in semi-leptonic decays. A similar comparison is done, see Table XVII, fitting only data relative to $D_{1/2}$ mesons, measured in semi-leptonic decays (in [5] measurements of non-leptonic transitions are not used). We have also modified our code to use the zero width formulation of our expressions as done in [5].

analysis	$\tau_{3/2}^{eff.}$	$\sigma_{3/2}^2$	$\hat{\tau}_1(CeV)$	$\hat{\tau}_2(GeV)$	χ^2/NDF
[5]	0.40 ± 0.04	1.6 ± 0.2	-0.5 ± 0.3	2.9 ± 1.4	2.4/4
our code	0.41 ± 0.06	1.60 ± 0.25	-0.66 ± 0.42	$5. \pm 2.$	1.8/3

TABLE XVI. Comparison between the values of fitted parameters obtained in [5] and with our own code, modified to be similar to the previous analysis and using the same input measurements.

analysis	$\tau_{1/2}^{eff.}$	$\sigma_{1/2}^2$	$\hat{\zeta}_1$	χ^2/NDF
[5]	0.35 ± 0.11	0.2 ± 1.4	0.6 ± 0.3	9.1/4
our code ($\Gamma(D_{1/2}) = 0$)	0.37 ± 0.11	0.26 ± 1.23	0.23 ± 0.31	7.0/3
our code ($\Gamma(D_{1/2}) \neq 0$)	0.30 ± 0.18	-1.6 ± 3.2	0.45 ± 0.28	6.0/3

TABLE XVII. Comparison between the values of fitted parameters obtained in [5] and with our own code, modified to be similar to the previous analysis. In the third line, values are obtained using the physical widths for the broad $D_{1/2}$ resonances.

Very similar results are obtained in the two analyses when considering zero width resonances. In the third line, obtained using the physical resonance widths, the central value of the IW function slope comes out negative, which is unexpected and inconclusive because the corresponding uncertainty is large. From all fits, with or without a finite resonance width, it can be concluded that data are not able to measure really this slope.

2. The main difficulty of the *LLSWB* analysis

Values obtained in this way, for $\tau_{1/2}^{eff.}(1)$ and $\tau_{3/2}^{eff.}(1)$ are compatible. This comes simply from the fact that the measurement $\mathcal{B}(\overline{B}^0 \rightarrow D_0(2300)^+ \pi^-)$ is not included in [4, 5] analyses. Meanwhile, expectations from relativistic quark models and LQCD [9], obtained in the $m_{b,c} \rightarrow \infty$ limit are very different with $\tau_{1/2}(1) \ll \tau_{3/2}(1)$.

If one assumes factorization ($a_1 = 1$), the branching fractions of the NL $\overline{B} \rightarrow D_{1/2}$ Class I decays predicted in *LLSWBi* are, at present, higher than the measured values by at least four standard deviations (when inclu-

ding the two channels)

This is illustrated in Section VIII A, Table XII, where we compare expectations from our model and from the *LLSWBi* analysis, for non-leptonic Class I $\bar{B} \rightarrow D_{1/2}$ decays.

Then we show that it is possible to fit data in a way which satisfies factorization for narrow and broad states and which is compatible with present theoretical expectations.

Annexe D: A summary of how the *LLSWBi* analysis differs from the *LLSWB* one and from our model

The *LLSWBi* analysis uses the same hypotheses as *LLSWB* does but, to make it directly comparable with our model we use the same input measurements and the same constraints from theory, when possible.

LLSWBi differs from our model by the following points :

- constraints from factorization are ignored in the production of $D_{1/2}$ mesons ;
- possible contributions from $D_V^{(*)}$ decays are ignored ;
- semi-leptonic branching fractions, $\mathcal{B}(\bar{B}^0 \rightarrow D_{1/2}^+ \ell^- \bar{\nu}_\ell)$, are taken from the last column of Table IV. It can be noted that the uncertainty taken for $\mathcal{B}(\bar{B}^0 \rightarrow D_1(2430)^+ \ell^- \bar{\nu}_\ell)$ is three times larger than

the one assumed in [4, 5] to account for the fact that the corresponding central value is obtained from an average of not compatible experimental results (the factor three is evaluated using the usual PDG recipe to scale uncertainties in this situation) ;

- no constraint is used on $\tau_{1/2}^{eff.}$;
- the measured fractions, in several w bins, attributed by Belle [8], to the $\bar{B}^0 \rightarrow D_0(2300)^+ \ell^- \bar{\nu}_\ell$ decay distribution are used ;

Because *LLSWBi* violates factorization in $D_0(2300)$ production and theoretical expectations for $\tau_{1/2}(1)$ it cannot be considered as a possible alternative to our model. We simply mean to illustrate the large expected differences between our model and previous analyses that can be confronted with data, when available.

1. Expected values for $\mathcal{B}(\bar{B}^0 \rightarrow D_i^{**,+} \ell^- \bar{\nu}_\ell)$

Expected values for semi-leptonic branching fractions, with a light or the τ lepton, in *LLSWBi*, are given in Table XVIII. As expected, they differ mainly from those quoted in Table XIII on the production of $D_{1/2}$ mesons and are now similar to those obtained for $D_{3/2}$ mesons. Values obtained in this approach, are essentially identical with the input values given in Table IV. Therefore estimates for the $D_1(2430)$ are quite inaccurate.

channel	e or μ $\times 10^3$	τ $\times 10^4$	$\mathcal{R}_{D^{**}}$ (%)
$\mathcal{B}(\bar{B}^0 \rightarrow D_2^{*+} \ell^- \bar{\nu}_\ell)$	3.16 ± 0.30	$1.90 \pm 0.27 \pm .07$	$6.01 \pm 0.49 \pm 0.19$
$\mathcal{B}(\bar{B}^0 \rightarrow D_1^+ \ell^- \bar{\nu}_\ell)$	6.40 ± 0.44	$6.19 \pm 0.56 \pm 0.15$	$9.67 \pm 0.62 \pm 0.24$
	$\times 10^4$	$\times 10^5$	(%)
$\mathcal{B}(\bar{B}^0 \rightarrow D_0(2300)^+ \ell^- \bar{\nu}_\ell)$	$39.1 \pm 7.0 \pm 0.2$	$31.9 \pm 7.9 \pm 2.0$	$8.2 \pm 1.5 \pm 0.5$
$\mathcal{B}(\bar{B}^0 \rightarrow D_1(2430)^+ \ell^- \bar{\nu}_\ell)$	$17. \pm 15. \pm 2.$	$12.8 \pm 11.5 \pm 5.0$	$7.6 \pm 1.0 \pm 2.0$

TABLE XVIII. *LLSWBi* model : expected semi-leptonic branching fractions with a light or a τ lepton, and their ratio, for the individual D^{**} mesons. Only model systematic uncertainties are quoted.

2. Expected values for $\mathcal{B}(\bar{B}^0 \rightarrow D_i^{**,+} D_s^-)$

Values for $\bar{B}^0 \rightarrow D_{3/2} D_s^-$ branching fractions are essentially identical with those obtained in our analysis. On the contrary, for $D_{1/2}$ mesons, they differ by about an order of magnitude, as expected.

Annexe E: Acknowledgements

We would like to thank colleagues who have provided interest and help on various aspects of this analysis, namely, D. Becirevic, I. Bigi, B. Blossier, S. Descotes-Genon and S. Fajfer. This study has been triggered by G. Wormser who asked us some advice about the interest of measuring $\bar{B} \rightarrow D^{**} D_s^-$ decays to improve our knowledge on D^{**} production in \bar{B} decays.

channel	value \pm fit	model
$\mathcal{B}(\overline{B}^0 \rightarrow D_2^{*+} D_s^-) \times 10^4$	5.7 ± 0.7	0.7
$\mathcal{R}_{D_2^*}^{\tau, D_s}$	0.34 ± 0.06	0.03
$\mathcal{B}(\overline{B}^0 \rightarrow D_1^+ D_s^-) \times 10^4$	12.3 ± 3.2	1.3
$\mathcal{R}_{D_1}^{\tau, D_s}$	0.50 ± 0.12	0.01
$\mathcal{B}(\overline{B}^0 \rightarrow D_0(2300)^+ D_s^-) \times 10^4$	16.0 ± 4.1	3.0
$\mathcal{R}_{D_0(2300)}^{\tau, D_s}$	0.20 ± 0.03	0.04
$\mathcal{B}(\overline{B}^0 \rightarrow D_1(2430)^+ D_s^-) \times 10^4$	5.3 ± 4.5	3.2
$\mathcal{R}_{D_1(2430)}^{\tau, D_s}$	0.24 ± 0.04	$^{+0.54}_{-0.12}$

TABLE XIX. *LLSWBi model*: $\mathcal{B}(\overline{B}^0 \rightarrow D_i^{*+, +} D_s^-)$ branching fractions, and their ratio, to corresponding semi-leptonic decays with a τ lepton. Only model systematic uncertainties are quoted.

-
- [1] A. K. Leibovich, Z. Ligeti, I. W. Stewart and M. B. Wise, Phys.Rev.Lett. 78 (1997) 3995, (hep-ph/970321)
- [2] A. Le Yaouanc, J.-P. Leroy and P. Roudeau, Phys. Rev. D 99 (2019) 073010, (hep-ph/1806.09853)
- [3] A.K. Leibovich, Z. Ligeti, I.W. Stewart and M.B. Wise, Phys. Rev. D **57** (1998) 308, (hep-ph/9705467).
- [4] F.U. Bernlochner and Z. Ligeti, Phys. Rev. D **95** (2017) 014022, (arXiv:1606.09300).
- [5] F.U. Bernlochner, Z. Ligeti, and D.J. Robinson, Phys. Rev. D **97** (2018) 075011, (arXiv:1711.03110).
- [6] Y. Amhis *et al.* [HFLAV], Eur. Phys. J. C **77** (2017) 895, (arXiv:1612.07233).
- [7] M. Tanabashi *et al.* (Particle Data Group), Phys. Rev. D **98** (2018) 030001.
- [8] D. Liventsev *et al.* [Belle Collaboration], Phys. Rev. D **77** (2008) 091503.
- [9] B. Blossier *et al.* [European Twisted Mass Collaboration], JHEP **0906** (2009) 022, (arXiv:0903.2298).
- [10] S. Godfrey and N. Isgur, Phys. Rev. D 32 (1985) 189
- [11] J.D. Bjorken, I. Dunietz and J. Taron, Nucl. Phys. 371 (1992) 111 (SLAC-PUB-5586).
- [12] A. Le Yaouanc, L. Oliver and J.-C. Raynal, Phys. Rev. D 69 (2004) 094022 (hep-ph/0307197).
- [13] N. Uraltsev, Phys. Lett. B 501 (2001) 86 (hep-ph/0011124).
- [14] A. Le Yaouanc, V. Morénas, L. Oliver, O. Pène and J.-C. Raynal, Phys. Rev. D **56** (1997) 5668 (hep-ph/9706265).
- [15] I.I. Bigi, B. Blossier, A. Le Yaouanc, L. Oliver and O. Pene, Eur.Phys.J.C 52 (2007) 975 (arXiv:0708.1627).
- [16] D. Becirevic, A. Le Yaouanc, L. Oliver, J.-C. Raynal, P. Roudeau and J. Serrano, Phys.Rev.D 87 (2013) 054007 (arXiv:1206.5869).
- [17] I. Bigi, M. Shifman, N.G. Uraltsev and A. Vainshtein, Phys. Rev. D 52 (1995) 196 (hep-ph/9405410)
- [18] P. Gambino, T. Mannel and N.G. Uraltsev, JHEP 10 (2012) 169, (arXiv:1206.2296)
- [19] N. Isgur and M.B. Wise, Phys. Rev. D43 (1991) 819.
- [20] M. Neubert, Phys. Rept. 245 (1994) 259 (hep-ph/9306320)
- [21] M. Beneke, G. Buchalla, M. Neubert and C.T. Sachrajda, Nucl.Phys.B 591 (2000) 313 (hep-ph/000612)
- [22] J.D. Bjorken, Nucl. Phys. B (Proc. Suppl.) 11, 325 (1989).
- [23] K. Abe *et al.* [Belle Collaboration], ICHEP04 11-0710, (hep-ex/0412072).
- [24] B. Aubert *et al.* [BaBar Collaboration], Phys. Rev. Lett. **100** (2008) 151802 (arXiv:0712.3503).
- [25] A. Vossen *et al.* [Belle Collaboration], Phys. Rev. D **98** (2018) 012005 (arXiv:1803.06444).
- [26] J.A. Bailey *et al.* [MILC Collaboration], Phys. Rev. D **92** (2015) 034506 (arXiv:1503.07237).
- [27] I. Caprini, L. Lellouch, and M. Neubert, Nucl. Phys. B **530** (1998) 153 (hep-ph/9712417).
- [28] S. Fajfer, J.F. Kamenik, and I. Nisandzic, Phys. Rev. D **85** (2012) 094025 (arXiv:1203.2654).
- [29] F. Jugeau, A. Le Yaouanc, L. Oliver, and J.-C. Raynal, Phys. Rev. D **72** (2005) 094010 (hep-ph/0504206).
- [30] This study was initiated following a proposal from G. Wormser.
- [31] C. S. Kim, Y. Kwon, J. Lee and W. Namgung, Phys. Rev. D **63** (2001) 094506 (hep-ph/0010157).
- [32] B. Chen, K.-W. Wei, X. Liu and T. Matsuki, Eur. Phys. J. C 77 (2017) 154 (arXiv:1609.07967)